E7.4-1 0.0 9 7

CR-136088

Σ
ENVIRONMENTAL
RESEARCH INSTITUTE
OF MICHIGAN

FORMERLY WILLOW RUN LABORATORIES. THE UNIVERSITY OF MICHIGAN

P. O. BOX 618 • ANN ARBOR • MICHIGAN • 48107   PHONE (313) 483-0500

INFRARED AND OPTICS DIVISION   20 November 1973
TECHNOLOGY APPLICATIONS   193300-31-L

National Aeronautics and Space Administration
Goddard Space Flight Center
Greenbelt Road
Greenbelt, Maryland 20771

Attention: Mr. E.F. Szajna, Code 430

Contract: NAS5-21783

Subject: Seventh Bimonthly (Type I) Report for Period Covering
            1 September 1973 - 31 October 1973

Dear Sir:

    The enclosed material comprises the seventh (7th) bimonthly technical
report for contract NAS5-21783, which describes the progress for the ten
tasks of the Environmental Research Institute of Michigan program for the
subject period. It is noted that this report covers the 15th and 16th
months of the contractual period, which is the eighth bimonthly period.
The required financial reports 533M and 533Q are submitted separately
from ERIM's accounting department. The work on this contract is performed
in the Radar and Optics Division (Task IV only) under the direction of
Dr. L. J. Porcello and in the Infrared and Optics Division (for the other
nine tasks) directed by Mr. R. R. Legault.

    Principal investigators for each task are listed in each subsection
of this report for the ten tasks. A summary listing of the tasks by
number, principal investigator and short title is provided as an attach-
ment to this letter. Titles of papers produced during this reporting
period and their authors also are listed as an attachment to this
letter.

    The status, principal activities and accomplishments of the various
tasks for this reporting period are noted here in summary form.

    TASK I - The new technique for determining water depth has been
given preliminary tests on parts of the frame 1089-16090 (Green Bay,
Wisconsin--Michigan area). Northern Lake Michigan tapes are available
for further tests; Puerto Rico test site tapes have not yet been
received.

ΣERIM

TASK II - A thirteen category recognition map of part of Yellowstone National Park is being checked by Dr. Harry Smedes, U.S.G.S. Work on the final report is underway.

TASK III - It has now been determined that ERTS overpasses of 16 February 1973 and 21 June 1973 will provide the principal data base for this task. Tapes for the first date are on hand. Two phases are in process for the test site - determination of atmospheric effects and recognition mapping.

TASK IV - In accordance with shift of the project effort to study of lake shore flooding, visual analysis of remote sensing data sources (aerial photos, ERTS frames, and S/L Radar) is being conducted. Mapping is in process. Usefulness of multi-frequency remote sensing sources is clearly indicated. Final report work is underway.

TASK V - Recognition processing of ERTS data for an Oakland County, Michigan, area has been continued by use of likelihood ratio processing in contrast to the previous work using level slicing techniques. A few problems were encountered due to clouds and non-homogeneous ground cover for selected training areas. The 7 June 1973 ERTS frame for the test site area, 1319-15474, is cloud free and better location of training sets will be employed for this frame. A digital recognition map for the test site area is included in this report, which is based on 1067-15465 (28 September 1972).

TASK VI - Most of the high speed processing, utilizing the ERIM-SPARC system on the previously converted to analog form ERTS tapes, has been completed for the Lake Ontario Basin. Eight targets were identified in this processing. Each selected target required about 1.5 hours for processing the 32,000 sq. mile area, portions of 8 ERTS frames for the Basin. Solutions of signature extension problems encountered are described. Figures included with this report show the video recognition of the area processed and an example of the processing results for one target, Surface Water.

TASK VII - This task is using an intensive study area located South-West of Lansing, Michigan, and a large extensive area of several counties in south central Michigan. Recently, for 6 September 1973, ERTS-1 data and A/C underflight data were obtained for a 4-mile flight line that included the Willow Run airport. Signature extension has been investigated in relation to a tree covered area in going from Day 1 to Day 2 ERTS-1 classification results; an empirical procedure and a theoretical procedure were used to adjust Day 1 signatures. Digital maps are presented in this report to show the results. An appendix presents some calibration results for the Bendix RMPI (Radiant Power Measuring Instrument).

ΣERIM

ERTS PROGRAM SUMMARY

Under Contract NAS5-21783

TASK	PRINCIPAL INVESTIGATOR	MMC #	UN #	SHORT TITLE
I	Polcyn	063	200	Water Depth Measurement
II	Thomson	077	621	Yellowstone Park Data
III	Thomson	137	636	Atmospheric Effects (Colorado)
IV	Bryan	072	201	Lake Ice Surveillance
V	Sattinger	086	225	Recreational Land Use
VI	Polcyn	114	635	IFYGL (Lake Ontario)
VII	Malila Nalepka	136	612 178	Image Enhancement
VIII	Wezernak	081	625	Water Quality Monitoring
IX	Horvath	079	606	Oil Pollution Detection
X	Vincent	075	422	Mapping Iron Compounds

LIST OF CURRENT PAPERS FROM THE TASKS

TASK	TITLE
VII	"Correlation of ERTS Data and Earth Coordinate Systems" by William A. Malila, Ross H. Hieber, and Arthur F. McCleer, was presented at the Purdue Conference on Machine Processing of Remotely Sensed Data, W. Lafayette, Indiana, 16-18 October 1973.
X	"Spectral Ratio Imaging Methods for Geological Remote Sensing from Aircraft and Satellites", by Robert K. Vincent, was presented at the American Soc. of Photogrammetry Symposium on Management and Utilization of Remote Sensing Data. 29 October-1 November 1973, at Sioux Falls, South Dakota, and appears in the Proceedings, pages 377-397.
X	"Ratio Techniques for Geochemical Remote Sensing", by Robert K. Vincent, was presented at the Symposium--Remote Sensing in Arid Lands, Tucson, Arizona, 14-16 November 1973.

ΣERIM

Seventh Type I Progress Report - 1 September 1973 - 31 October 1973
Task I - Water Depth Measurement - 1388
F.C. Polcyn, UN 200, MMC 063

The new water depth technique described in the previous Progress
Report has been implemented and tested with ERTS data for Northern Lake
Michigan, near the mouth of Green Bay. Two areas were selected from
ERTS frame 1089-16090 for processing: one along the east coast of the
Door Peninsula, and one covering the inlet to Green Bay from Point
Detour, Michigan to the tip of the Door Peninsula.

The combination of low sun elevation (30°) for this date
(20 October 1972) and relatively high water attenuation makes this
a "worst case" test for which water depth can be computed. The theoretical
maximum depth that could be computed for these data is about 2.8 meters.
Because of noise, variations in water quality, and gain differences
among the six detectors, the maximum depth actually mapped was 2 meters.

Depth charts were successfully produced for these two areas,
showing four categories of water depth: 0-1 m, 1-1.5 m, 1.5-2 m, and
over 2 m. Several shoals were observed in agreement with Lake Survey
charts of the area. The depth charts were produced with a one-step
process using minimal computer time.

Data tapes have since been received for Northern Lake Michigan with
a higher sun elevation. These will be processed in the next period to
determine maximum depths that can be measured with higher scene
illumination.

Imagery has been received for the Puerto Rico test site, for
18 October 1973. The data tapes for these frames (1087-14221 and
1087-14223) are on order, but have not yet been received.

⟩ERIM

Seventh Type I Progress Report - 1 September 1973 - 31 October 1973
Task II - Yellowstone National Park Data - 1398
F.J. Thomson, UN 621, MMC 077

Technical work on this task is nearly complete. Final display of
the thirteen category recognition map is now being prepared by Mead
Corporation (formerly Data Corporation), and the finished map is expected
by 10 December. Dr. Harry Smedes, U.S.G.S., is checking the accuracy
of the thirteen category map now, and his answers are expected by the
end of December.

A final report outline is now being prepared, and writing of the
final report will commence by the end of November. Certain sections
which Dr. Smedes will prepare for the final report will be integrated
in late December.

A presentation was made before the Land Use review panel at GSFC.
This presentation summarized the progress on this task of the contract
up to 15 October. Favorable comments were received from the committee.

>ERIM

Seventh Type I Progress Report - 1 September 1973 - 31 October 1973
Task III - Atmospheric Effects in ERTS-1 Data - 1410
F.J. Thomson, UN 636, MMC 137

The general objectives of this task are to determine the effects of the atmosphere on the ability of pattern recognition devices to classify terrain objects and to assess their significance relative to other factors affecting the automatic classification of terrain objects. The project is a cooperative one between ERIM personnel, Dr. Harry Smedes of the U.S.G.S., and Mr. Roland Hulstrom of Martin-Marietta Corporation.

Recent conversation with Mr. Hulstrom has ascertained that funds designated for the collection of atmospheric measurements coincident with ERTS overpasses are now exhausted. Preparations made for data collection on 8 October had to be cancelled due to overcast sky conditions. As a result, two sets of atmospheric measurements, made in conjunction with ERTS overpasses of 16 February and 21 June 1973, will constitute the basis for fulfilling the objectives of this task. ERTS CCTs for 16 February are presently in hand. Tapes for the 21 June data are on order.

This task can be divided into two separate phases of activity: the determination of atmospheric effects and recognition mapping of the test site. Progress in each phase is reported separately as follows:

Atmospheric Effects

In an effort to arrive at some idea of the magnitude of radiance variations to be expected in ERTS data as a result of changes in base elevation, preliminary theoretical calculations and empirical observations were made using visibility conditions reported by a weather reporting station at Colorado Springs and ERTS data respectively for the date of 20 August 1972.

Theoretical calculations were made with a radiative transfer model developed by Dr. R.E. Turner [1] of ERIM. A horizontal visibility of 160 km. reported by Colorado Springs at the time of ERTS overpass on 20 August 1972 was used to specify atmospheric state. Since no measured optical depth parameters were available for this date, the use of horizontal visual range enables identifying the total optical depth by referencing a standard atmospheric aerosol profile for use in the calculations. To simulate changes in optical depth caused by variations in atmospheric path length (as a result of varying base elevation), the standard atmospheric Rayleigh term of optical depth was adjusted for base elevation increases by multiplying the Rayleigh optical depth by the ratio of the barometric pressure at altitude to the barometric pressure at sea level. The aerosol term of the optical depth was unchanged.

Model calculations were made for base elevations of 7K, 9K, 11K, and 13K ft. These base elevations span the range of elevations found in the test site. Results indicated little difference in the total amount of spectral irradiance incident on an object at 7K ft and one at 13K ft. Although atmospheric transmittance increased with decreasing path length (increasing base elevation) for each of the four MSS bandwidths, the percentage of diffuse irradiance decreased by a similar amount. As one would expect, the changes were greatest for MSS 4. For this bandwidth, transmittance increased by 1.5% from 7K to 13K ft while the percentage of diffuse irradiance relative to the total was seen to decrease by 1.6% for the same base elevation increase. Thus, for the atmospheric state hypothesized on the basis of reported visibility conditions, computed variations in spectral irradiance for the range of base elevations existing in the test site seem to be slight since increases in direct illumination (as affected by transmittance) are similarly offset by decreases in diffuse illumination. In like manner, computed total and path radiance for objects of low reflectance had negligible variations for assumed background contrast ratios at different base elevations.

A desire to substantiate the theoretical calculations prompted the following empirical procedure with ERTS data collected on the same day. Mean signal values in each MSS channel for each of nine water reservoirs (see table 1) were converted to radiance using conversion values listed in Table G.2-2, page G-14 of the Data Users Handbook. Radiance values for the reservoirs (ranging in elevation from 7K to 11.7K ft) were then plotted as a function of base elevation (see figures 1-4). The vertical bar on each figure represents the estimated magnitude of radiance change for a 1% change in object reflectance using the irradiance and trans-mittance conditions computed with the model.

TABLE 1. Water reservoirs in test site for which radiance values were computed from ERTS data.

Number	Name	Elev. (ft)
1	Elevenmile Canyon Reservoir	8,600
2	Lake George	8,000
3	Cheesman Lake	7,000
4	Monument Reservoir	8,900
5	South Catamount Reservoir	9,300
6	Reservoir No. 8	11,700
7	Bison Reservoir	10,500
8	Wright's Reservoir	8,100
9	Skagway Reservoir	8,900

Figure 1

CRIPPLE CREEK 20 AUGUST 1972

TOTAL RADIANCE VS. BASE ELEVATION
FOR 9 WATER BODIES (ERTS BAND 4)

$L \, (mw/cm^2 \, sr \, \mu m)$

Figure 2

CRIPPLE CREEK 20 AUGUST 1972

TOTAL RADIANCE VS. BASE ELEVATION
FOR 9 WATER BODIES (ERTS BAND 5)
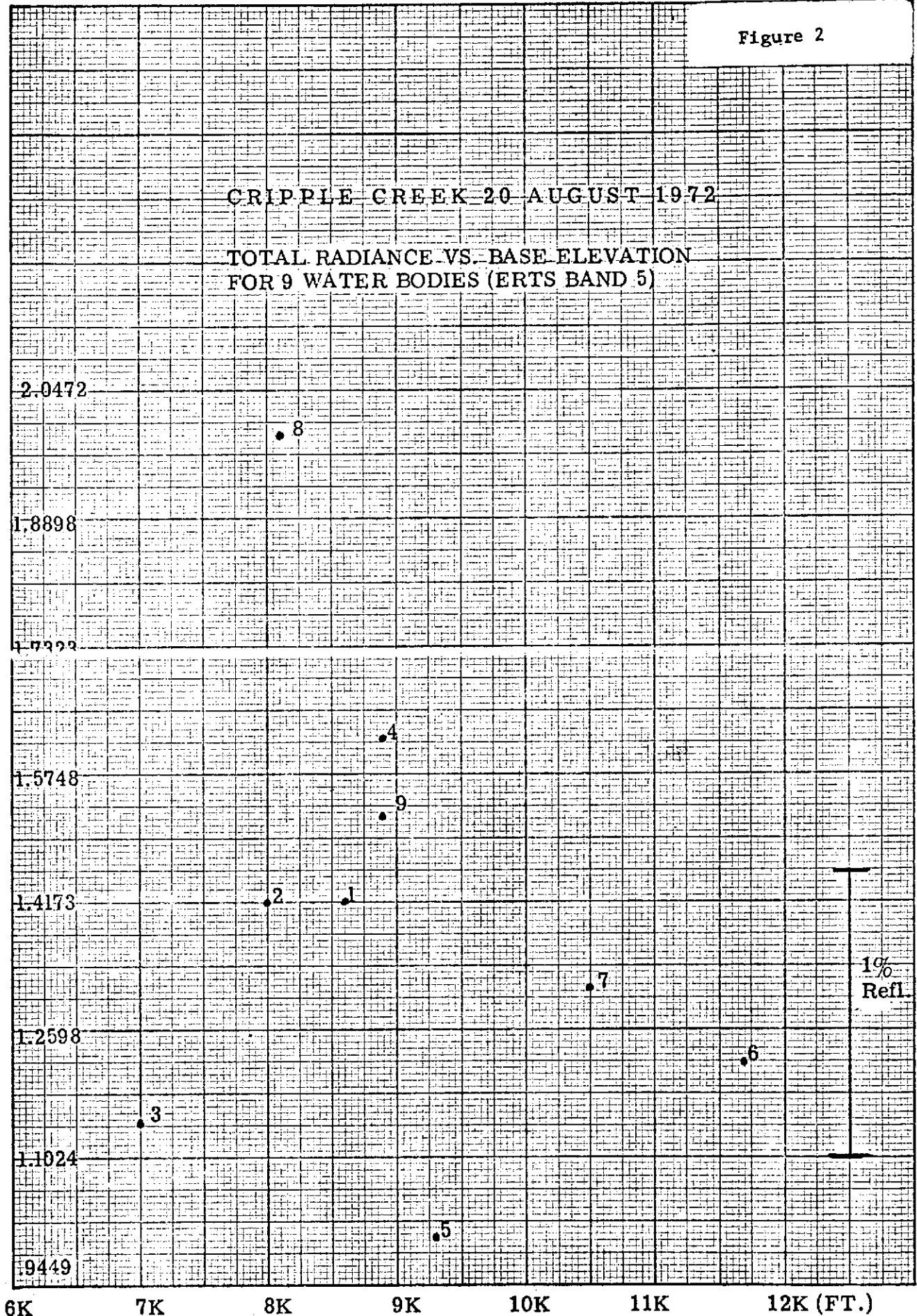
Figure 3

CRIPPLE CREEK 20 AUGUST 1972

TOTAL RADIANCE VS. BASE ELEVATION
FOR 9 WATER BODIES (ERTS BAND 6)

$L \ (mw/cm^2 \ sr \ \mu m)$

20 X 20 TO THE INCH   46 1240
7 X 10 INCHES   MADE IN U.S.A.
KEUFFEL & ESSER CO.

.9701

.8315

.6929

.5543
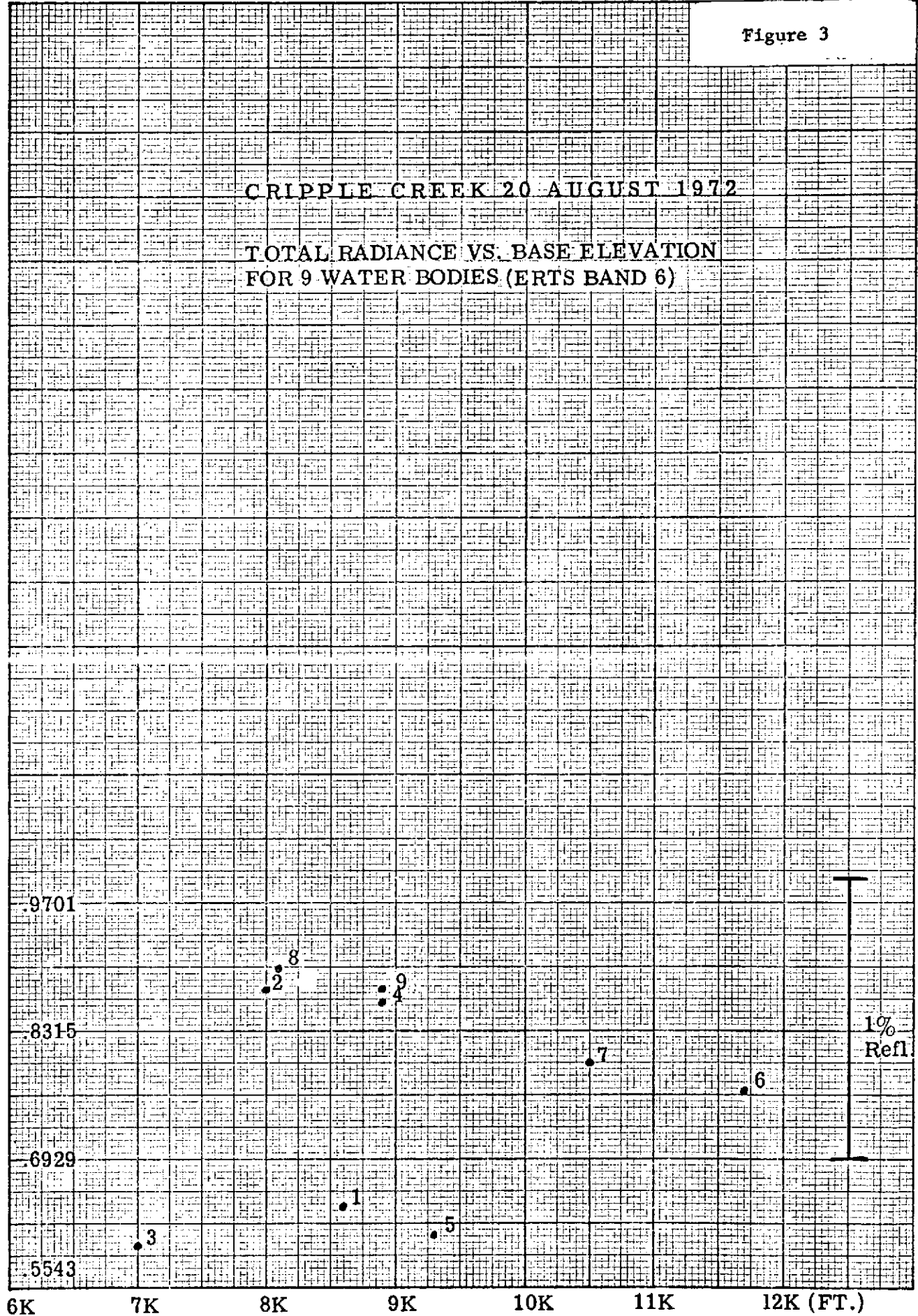
6K   7K   8K   9K   10K   11K   12K (FT.)

1%
Refl.

Figure 4

CRIPPLE CREEK 20 AUGUST 1972

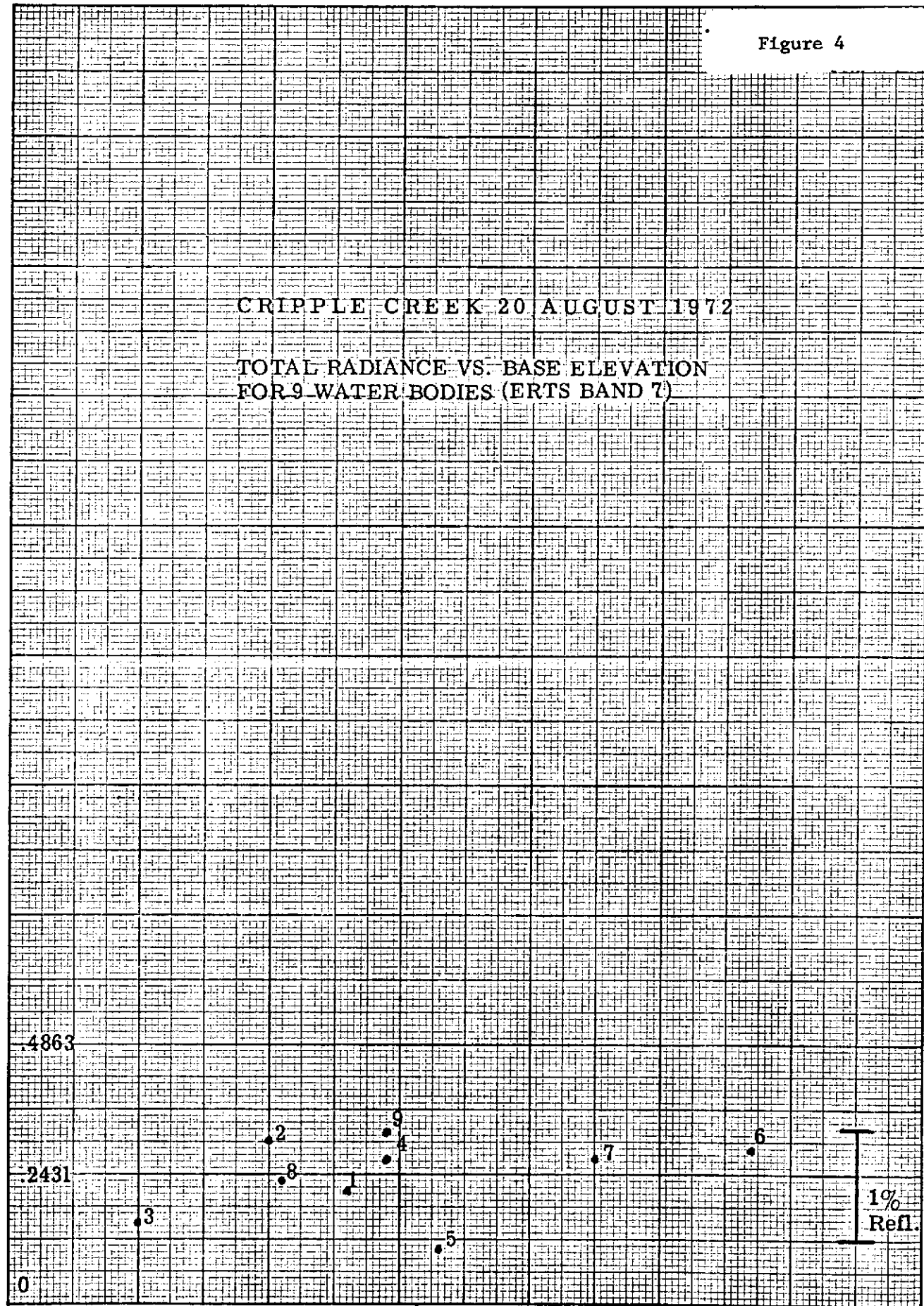TOTAL RADIANCE VS. BASE ELEVATION
FOR 9 WATER BODIES (ERTS BAND 7)

$L \ (mw/cm^2 \ sr \ \mu m)$

.4863

.2431

0

6K   7K   8K   9K   10K   11K   12K (FT.)

1%
Refl.

Water reservoirs were selected because of their common orientation to the ERTS sensor. As can be seen in figures 1-4, there is a lack of obvious correlation between the water radiance in all ERTS-MSS bands and base elevation. This suggests that the natural variability of reflectance between water bodies exerts more influence over the observed radiance than variations in atmospheric path radiance and transmission caused by differing base elevations. We conclude that water quality variations between lakes in the test site exert greater influence over water spectral radiance signatures than variations in base elevation. This conclusion is obviously conditional on there being 160 km visibility or greater.

Further study with ERTS data of 21 June will compare the use of measured optical depth parameters against horizontal visual range estimates. Comparisons of measured and predicted irradiance levels at the ground will be made.

Inspection of ERTS data from a 16 February 1973 overpass (a snow-covered scene) has indicated that the radiance of snow exceeds the dynamic range of the MSS for bands 4 and 5 -- the result being maximum integer levels recorded for all resolution elements over snow.

This result is supported by Hulstrom's field measurements of 16 February, but could not have been predicted in advance. Signals in band MSS-6 appear to be clipped for some of the six detectors and not for others--a result at variance with Hulstroms field measurements, which indicate that snow signals probably should be clipped. In band MSS-7, snow signals are not clipped, and we have Hulstrom measurements of snow radiance. This may permit a calibration of band MSS-7. Since the atmospheric effects are negligible because of the good visibility and high elevation, Hulstrom's radiance values should very closely agree with the radiance from the scanner. Turner's model can calculate corrections for atmosphere if a more precise calibration is desired. This work will be continued during the next period.

Recognition Mapping

The data of 20 August 1972 (Frame 1028-17135) provides good coverage of the test site and is being used for the initial recognition map. Sixteen categories of terrain classes were preliminarily defined as being significant for classification by Dr. Smedes. Training areas for each category were initially delineated on an eight level digital graymap of band 5 that depicted every second pixel in every second scan line. This effort was provided by an assistant of Dr. Smedes at Colorado State University with the aid of high altitude color photography and U.S.G.S. topographic map sheets. Evaluation of resulting signatures for each category showed excessive statistical variability in many cases, indicating an inability to precisely locate training areas. Portions of the

∑ERIM

test site have therefore been remapped to allow the display of each pixel into one of 17 quantum levels. Delineation of new training areas is now in progress.

Once accurate signatures are established, further statistical analyses will attempt to determine their suitability for accurate classification of the test site. Variations among signature means (within channel and between channels) will be related to the physical characteristics of the training sets, slope and aspect variances, and if possible, to varying base elevation. However, the inherent variability of natural materials and varying slope and aspect may preclude any correlation between signatures of terrain classes and base elevation. The combination of some preliminarily defined categories and definition of additional categories is also to be considered. The final set of signatures will be used to classify the test site according to the maximum likelihood ratio criterion.

Activity during November and December will be primarily concerned with the study of atmospheric effects for the date of 21 June 1973. Theoretical calculations made with the radiative transfer model will be compared with actual measurements made on the site.

Further activity with recognition mapping will await the accurate designation of training areas.

REFERENCES

1. "Importance of Atmospheric Scattering in Remote Sensing," by R. Turner, W. Malila, and R. Nalepka. Proceeding of the 7th International Sympsoium on Remote Sensing of Environment, Willow Run Laboratories, The University of Michigan, Ann Arbor, 1971.

ΣERIM

Seventh Type I Progress Report - 1 September 1973 - 31 October 1973
Task IV - Lake Ice Surveillance - 1406
M. Leonard Bryan, UN 201. MMC 072

Following the change in the work statement as discussed in the
previous Type I report, visual analysis using the several data sources
(aerial photography, enlarged ERTS (I) frames and X/L Radar) have been
initiated. This analysis is based primarily on the preparation of
overlays, the mechanical measuring of areas (by planimeter) and the
tabulation of the types of information, relative to flooding, which
are available from each of the several data sources. The philosophical
approach that there is a need to conduct this work based primarily on
non-machine types of analysis, is being maintained. Thus, we continue
to be oriented toward the development and substantiation of near
real-time applications of both the ERTS (I) and the radar imagery--
applications which can be easily conducted by individuals having a
minimum of remote sensing interpretation training and not having
ready access to automatic data processing tools.

Many investigators have previously noted that multifrequency remote
sensing, combining analysis of data from the optical and microwave
portions of the spectrum, was a powerful tool because the microwave data
supplement and complement the optical data. Although the mapping here is
incomplete and cannot be presented in this report, our work to
date further demonstrates the supplementary and complementary value of radar
data to ERTS data.

No reports have been presented during this reporting period. One
talk was presented: 24 October 1973, Goddard Spact Flight Center.
Water Resources Panel.

No changes in the standing order forms or submission of data
request forms were made during the reporting period.

It is planned to complete the visual analysis of the several data
sets which are available and present the final report for this project
at the termination of the contract on 11 December 1973.

Seventh Type I Progress Report - 1 September 1973 - 31 October 1973
Task V, Recreational Land Use - 1387
I. Sattinger, UN 225, MMC 086

Major effort during this reporting period was devoted to analyzing
the results of likelihood ratio processing of a 150 sq. km. area in
Oakland County. This is the same area previously mapped by edited
level slicing techniques and the same ERTS digital data (acquired on
28 September 1972) was used in the likelihood ratio mapping.

On 24 October 1973, the Principal Investigator made a presentation
of these results to the Land Use Discipline Panel at Goddard Space
Flight Center.

Selection of Training Sets

The final selection of training areas on which to base maximum
likelihood ratio processing included residential areas, sand and gravel
pits, forest areas, other vegetation-cover, and deep and shallow water
(see Table 1). Since the coverage was obtained near the end of the
growing season, very little bare soil is visible in the area. In
selecting these training sets, we experienced several difficulties which
somewhat limited the accuracy of our recognition mapping process. In
some cases, training areas were inadvertently chosen which were later
found to be covered by haze or clouds. The radiance in each of the four
bands was therefore somewhat brighter than that corresponding to the
underlying land or water surface. We encountered another difficulty in
selecting an area on the initial computer printout which coincided with
a known area recognized on an RB57 photograph. As a result, the surface
covered by the training set was not a homogeneous type of ground cover
in some cases. Because of the substantial size of forest and water areas,
suitable training sets were easily selected. In the case of types of
vegetative cover other than forest, homogeneous areas were not selected
and the training sets did not clearly distinguish major categories of
vegetation from each other, such as brush and grass.

In future processing, we will be able to improve our results by
working with a cloud-free frame acquired on 7 June 1973, so that contamin-
ation of the signatures by cloud cover will not occur. We will also adopt
improved methods of selecting homogeneous training areas based on accurate
geographic correlation of gray map and photograph.

Mapping Results

The recognition map prepared by maximum-likelihood processing is
shown in Figure 1. Symbols used are listed in Table 1.

ΣERIM

TABLE 1

TRAINING SETS

Training Set	Symbol	Elements	Hectares
Water, shallow or haze-covered	Blue *	1121	500
Water, deep	Blue M$	2318	1020
Soil; gravel	Red .	1899	839
Medium density residential	θ	3924	1730
Medium density residential (haze)	Red *	2714	1200
Medium density residential (haze)	Red X-	1780	785
Medium density residential (50% vegetation)	Red O	1512	668
Trailer park	Red M$	435	192
Mixed hardwood forest	M$	7821	3450
Transition (forest/grass)	*	3858	1700
Grass; upland brush	Green O	6478	2860
Grass; active cultivation	Green *	5902	2605
Golf course	Green X=	1835	810
Unclassified		35	15
Total		41632	18374

As indicated previously, a sizable area near the bottom of the test area was cloud covered, and small isolated clouds were distributed over other parts of the scene. The lower section of the picture was therefore mapped by symbols corresponding to urban or sand and gravel areas, which approach the clouds in brightness. Isolated clouds in other parts of the scene also appeared in the recognition map as soil or gravel and shadows caused by these clouds were mapped as water. These discrepancies are easily detected and accounted for in the overall checking of the area map.

Water Bodies

The signature of water bodies is sufficiently different from other types of surface that they are reliably recognized and mapped. Large bodies of water, such as lakes, are mapped with very little error, except at the shoreline where mixtures of land and water occur in individual pixels. Even bodies of water as small as a hectare in size are usually detected, although their shape is distorted by the grid structure of the map, and their exact area is subject to considerable error. In one area (near the left edge of Figure 1) a series of small ponds or lakes occurs, but only one of these lakes was detected. Examination of the photography indicated that the other lakes or ponds contained substantial amounts of vegetation or algae, which would have interfered with the recognition process.

Residential Areas

As indicated in the discussion of training sets, residential areas with little vegetative cover tend to be mapped as homogeneous areas similar to sand or bare soil. This situation would be approached for a trailer park. In areas containing substantial amounts of trees and lawn, the mapping consists of a mixture of light tones and various types of vegetation. Because of the mottled character of such residential areas, it would be difficult to select a single signature which would be consistently mapped in such areas. Residential areas with substantial vegetation cover have to be recognized not from single pixels but from textural analysis of a group of such pixels. The heterogeneous character of residential areas may provide a basis for distinguishing such areas from trailer parks, bare fields, sand and gravel pits, commercial and industrial areas, and for delineating the rural/urban boundary. Although residential areas are generally distinguishable from other types of land use, some confusion might occur for residential areas whose composition closely approximates either completely paved areas or completely vegetated areas.

Highways

The only highway which is clearly identified on the recognition map is a short section of I-75 at the extreme top of the map, which is represented by a linear distribution of various red symbols.
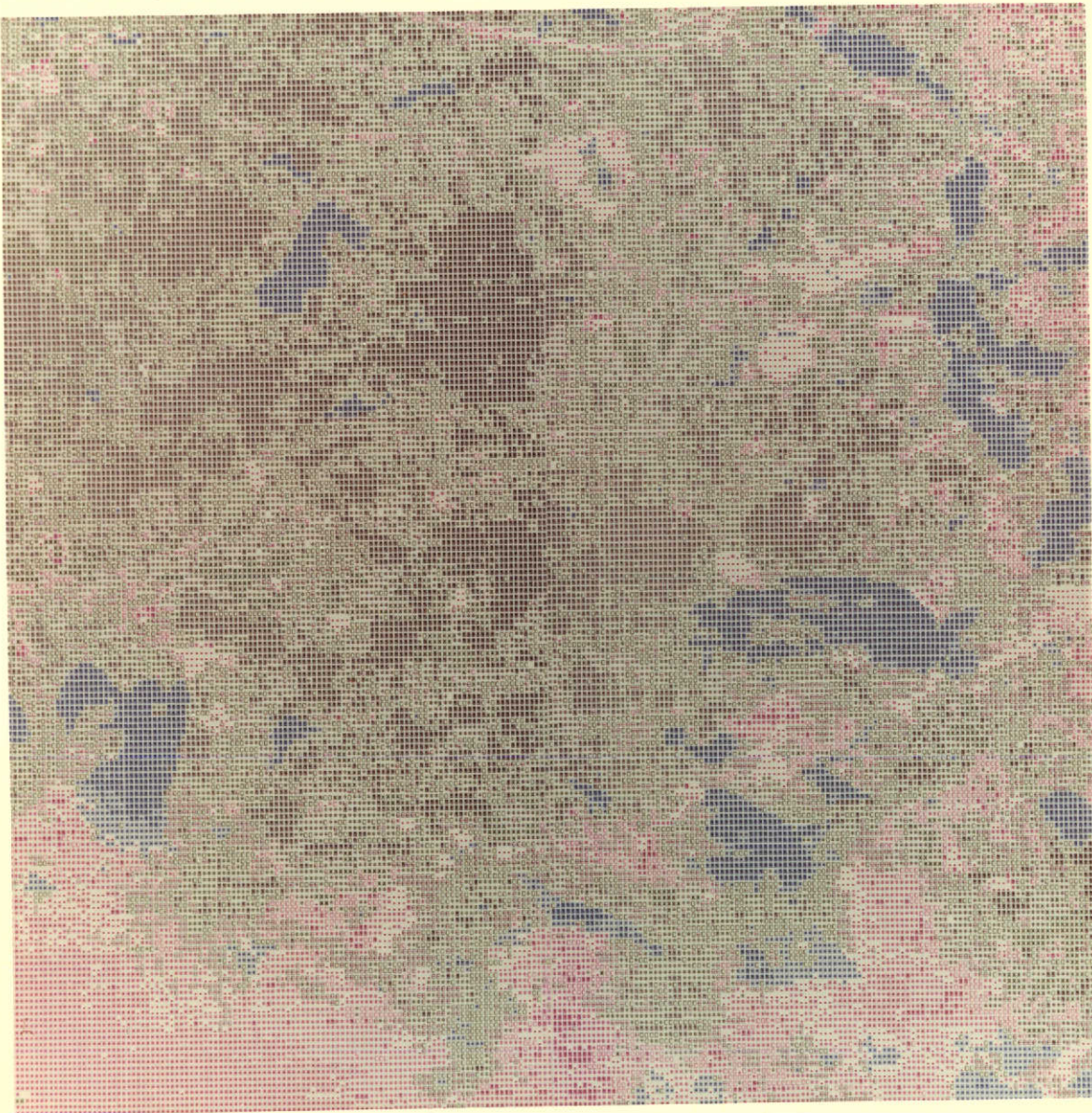
ERIM

FIGURE 1 - DIGITAL RECOGNITION MAP OF OAKLAND COUNTY TEST AREA

ΣERIM

Forested Areas

In the test area, the trees are predominantly deciduous, with the majority of the forest-covered areas consisting of mixed and lowland hardwoods. Two separate training sets were used to identify forests. The resulting training sets were consistently recognized as forest in the recognition map, confirming the estimate that these training sets were selected in areas of homogeneous forest cover.

A study of the signatures of the various vegetation classes indicates that the forest training set signatures were sufficiently different from other classes of vegetation that they should be distinguished with reasonable accuracy from all other vegetation. Visual comparison of the recognition map with aerial photography indicates a reasonably good correlation of location, size, and shape of wooded areas as small as 5 or 10 hectares. There may, however, be a tendency to map as forest some areas which have been designated in the vegetation map of Oakland County as upland brush.

No attempt was made in this recognition mapping process to distinguish among various communities or species of trees. There is little coniferous tree cover in the area studied, and suitable training sets for differentiation of major types were not easily available. For many studies of recreational land, such differentiation of tree types would be significant, and it is therefore planned in future work on this project to address this problem.

Other Vegetation

A check on the accuracy of recognition mapping of vegetation categories other than forest is difficult to accomplish in the area under study. The rural areas are characterized by great variability of surface cover and there are few homogeneous areas of sufficient size to be isolated for comparison with aerial photography.

A study of the signatures of training sets of other vegetation indicates that some of these signatures are reasonably distinguishable from each other. However, the selection of training sets did not provide a separation of vegetation into sufficiently clear-cut categories. Thus, the general mapping of other vegetation as a single group appears to be quite effective, but the distinction among individual categories is inconclusive at this time.

Accuracy Check

Because of the complexity of the test area, it is difficult to tie individual pixels in the recognition map to corresponding features on the higher-resolution photograph for purposes of checking accuracy. We found

that a suitable approach to the task of checking map accuracy, short of a
sophisticated computer-based registration procedure, is to compare the
shape and extent of sizable features on the map and photograph. The
recognized category can be checked against the intepretation of the feature
from the photograph. Also, smaller objects included in the larger feature
or close to it can be accurately located and identified in the recognition
map. General conclusions reached from this method of comparison have
been discussed above.

In addition, an accuracy check was performed on an East-West transect
taken through the northern part of White Lake and the large trailer park
several miles east which was used as the training set for one of the
urban classes (Red M$). This transect contains 227 pixels. The accuracy
of the digital map prepared by maximum likelihood ratio processing was
checked by comparing it to an RB57 color IR photograph of the area. A
similar accuracy check was performed on a land use map obtained by
conventional photointerpretation of the ERTS image of the same area.

In checking the digital map, the classification of the land, as
indicated by the digital symbols, was compared to the classification
obtained by photointerpretation of the corresponding strip on the
RB57 photograph. It was necessary to identify the area on the RB57
photograph corresponding to the transect and to maintain this
correspondence to the nearest pixel across the entire section. This was
a difficult task to perform, and any loss of exact registration would
affect the validity of the check procedure.

Table 2 shows the comparison of pixel classification from the two
sources.

Since the urban and vegetation areas were not clearly differentiated
by the training sets chosen, it was not considered practicable to check
the accuracy of mapping all categories. Instead, the matching data were
aggregated into the four major classes of water, urban, forest, and other
vegetation. When this was done for the digital map, the number of
matching pixels amounted to 208 out of 227, for an accuracy of 92%.

These results may be compared with the match of RB57 photography
against the same transect of a land use map prepared by photointerpretation
of ERTS imagery. For the same four classes of water, urban, forest,
and other vegetation, the number of matching pixels yielded a total of
169 out of 227 for an accuracy of 74%.

In comparing this latter result with the accuracy cited for digital
mapping, it should be kept in mind that this result was probably not the best
possible performance that can be expected from ERTS photointerpretation.
The imagery used for the purpose included the black and white transparencies
for Bands 5 and 7, and the color transparency of the same scene. If
improved products can be used for the photointerpretation, such as color

TABLE 2

ACCURACY COMPARISON

Pixels in Class Correctly Identified

Class	ERTS Photointerpretation (Percent)	ERTS Digital Mapping (Percent)
Water	89	89
Urban	44	74
Vegetation	92	97
Forest	52	92
Overall	74	92

$\sum$ERIM

imagery with better resolution, it should be possible to improve the accuracy rating above that noted. However, a significant advantage of digital mapping over ERTS photointerpretation probably accounts for some of the difference. Every pixel in the complete scene is analyzed by the digital processing, whereas with photointerpretation, realistic limitations on photointerpretation effort require the placing of boundaries around what appear to be homogeneous areas of land cover. For the complex scene characteristic of the area we are investigating, this grouping process of photointerpretation reduces the amount of detail which can be incorporated into the final product.

Future Work

Project effort during the next reporting period will be concentrated on two tasks. Signature data from ERTS frames acquired on 27 March 1973 and 7 June 1973 will be analyzed for areas in which good ground truth is available on tree species or communities and on wetland areas. This analysis will indicate the ultimate potential of ERTS computer processing for differentiating such areas. The second task will be to repeat the processing of the same test area in Oakland County previously analyzed using cloud-free data from the 7 June 1973 frame and improving the selection of homogeneous training areas.

ERIM

Seventh Type I Progress Report - 1 September 1973 - 31 October 1973
Task VI - IFYGL (Lake Ontario) 1384
F.C. Polcyn, UN 635, MMC 114

This two-month period saw the completion of most of the high-speed processing for the Lake Ontario Basin and the initiation of the parallel digital processing of the East and Middle Oakville Basin. Preliminary results of this processing were presented to the Environmental Panel during meetings at Goddard on 25 October. All ERTS data processing is on schedule and there are no current probelms with this task.

The ERTS data tapes previously converted to analog form were processed during this period using the ERIM-SPARC system--a special purpose likelihood-ratio image classifier. The speed of this system is such that ERTS-data comprising portions of 8 ERTS frames (32,000 sq. miles) were processed at the rate of 1 1/2 hours per target. First, the available data-tapes were edited to provide approximate delineation of the Lake Ontario Drainage Basin (See Figure 1; note that a small part of the basin is omitted at the right hand side of the figure). Eight targets, representing 8 hydrologically-significant terrain-classes, were printed out. These were subsequently mosaiced to produce a single image of each terrain class for the basin (e.g., Figure 2). Simultaneously, with the printing of each terrain class analog recognition counts were recorded digitally for each class. Since the total number of counts for the entire Basin had been previously established, the percentage of the basin occupied by each class was obtained.

In producing these terrain thematic maps from ERTS imagery a number of problems were overcome. The main problem was how to extend a single recognition signature for a single terrain type to a number of ERTS frames--not all of which were collected on the same day. Two types of preprocessing were involved in the solution to this problem--dark level subtraction and ratioing of ERTS bands. In dark-level subtraction, a discrete value which represented the signal-level for the darkest object in each ERTS frame was subtracted from each pixel, or scene element. This dark-level value was slightly different for each frame and was assumed to represent the D.C. effect of additive atmospheric path radiance and scanner calibration differences (from one day to the next). The ratio of two ERTS bands provided recognition criteria based on the relative spectral difference which occurs between each band, and not on the absolute signal levels. The ratio results were previously discussed (1).

Parallel digital processing is being coupled with the high-speed processing in an effort to better understand and validate the recognition results from the SPARC (see Figure 3). In this case, a small representative watershed (81 sq. miles) was selected for this accuracy test. The digital results are expected to provide empirical bounds for the classification accuracy of the thematic maps for the entire Basin. Also it is hoped that the results will contribute to efforts to develop a mathematical model of this watershed by the Ontario Ministry of the Environment.
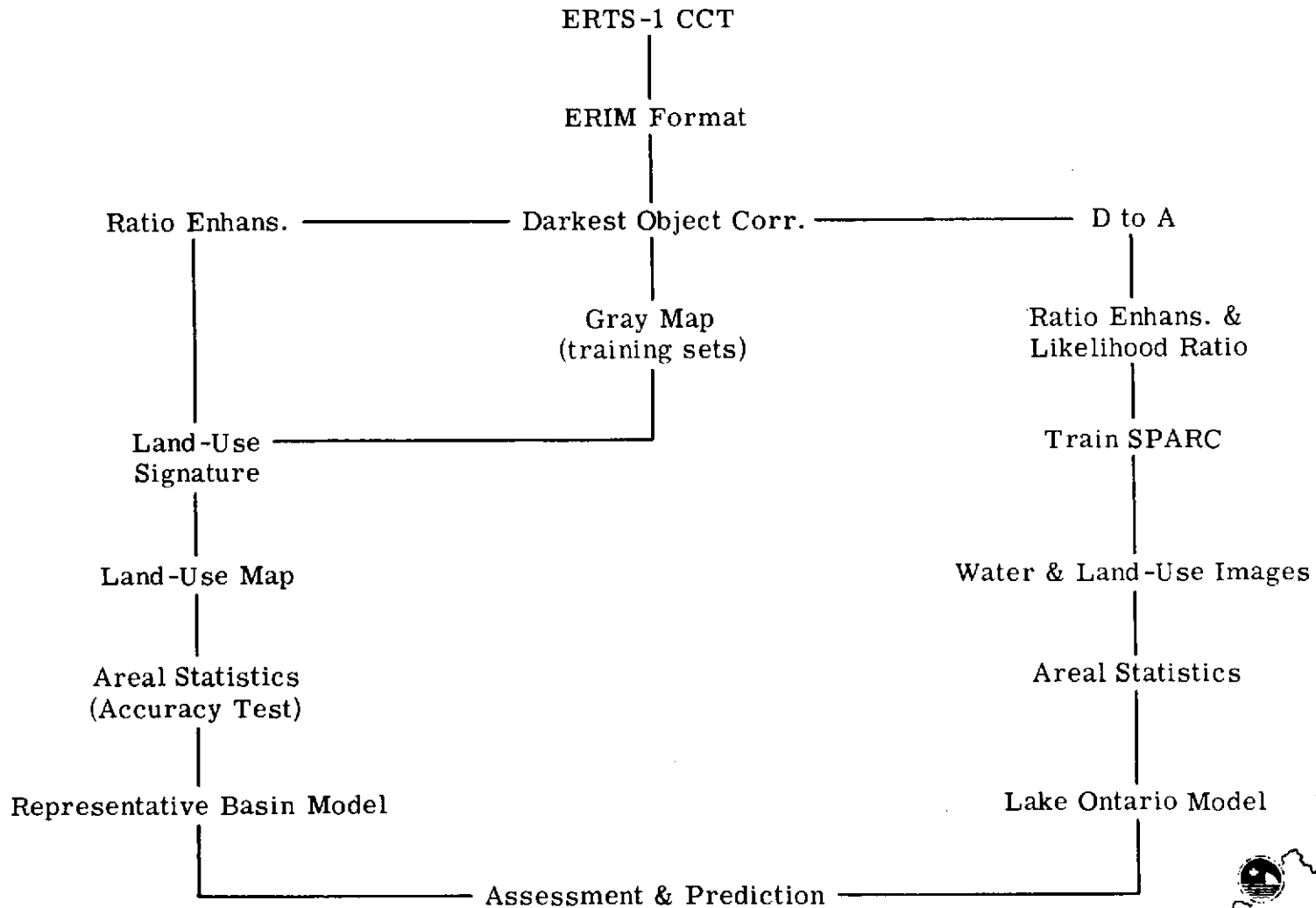
LAKE   ONTARIO   BASIN

PROCESSED   0.6 - 0.7 μm   IMAGE   AUGUST   19 - 21, 1972

FIGURE 1

SURFACE   WATER   MAP

ONTARIO   BASIN

AUGUST   1972

FIGURE 2

ERTS—IFYGL LAKE ONTARIO PROJECT

DATA PROCESSING

ERTS-1 CCT
|
ERIM Format
|
Ratio Enhans. ———————— Darkest Object Corr. ———————— D to A

Gray Map
(training sets)

Ratio Enhans. &
Likelihood Ratio

Land-Use ————————————
Signature

Train SPARC

Land-Use Map

Water & Land-Use Images

Areal Statistics
(Accuracy Test)

Areal Statistics

Representative Basin Model

Lake Ontario Model

———————— Assessment & Prediction ————————

ΣERIM

FIGURE 3

> ERIM

Seventh Type I Progress Report
Period: 1 September – 31 October 1973
W. A. Malila (UN612) & R. F. Nalepka (UN178), MMC 136
Task VII, Image Enhancement and Advanced Information Extraction Techniques

INTRODUCTION

Experience has been gained at ERIM over the past decade in computer processing and extraction of information from airborne multispectral scanner (MSS) data and in modeling atmospheric effects in received radiance signals. The general objective of Task VII is to adapt techniques existing at ERIM for their application to ERTS-1 data, to assess the applicability of these techniques by applying them to selected ERTS-1 data, and to identify any additional problems that might be associated with such processing of satellite multispectral scanner data. Three areas are to be studied: (1) compensation for atmospheric effects in ERTS-1 data, (2) preprocessing for improved recognition performance through signature extension, and (3) estimation of proportions of unresolved objects in individual resolution elements.

The intensive test site for this investigation is an agricultural area South-West of Lansing, Michigan, and the extensive test area also covers several other counties in South Central Michigan. A variety of agricultural crops and woodlots are in the intensive area. The primary crops are corn and wheat, with field beans, soybeans, and alfalfa also represented. The intensive test area is in an overlap region covered by ERTS-1 on two successive days of each 18-day cycle. Skies were clear on 25 August and ERTS data were collected. Simultaneous multi-altitude underflight coverage was obtained by the Michigan C-47 multispectral scanner aircraft, and ground-based measurements were made of spectral irradiance and sky radiance. RB-57 camera coverage of the region, obtained during June, was received in late September. A second RB-57 flight was made in mid-September, and its photography was received at the end of October. A second multispectral scanner aircraft mission was scheduled. Partial coverage was obtained in June 1973 and the site for the remaining lines was moved to the Willow Run Airport.

SIGNIFICANT RESULTS

Preprocessing techniques for signature extension were utilized to improve machine classification performance in using signatures from one day and applying them to data from another day over the same area with a different amount of atmospheric haze present. Both an empirical procedure and a theoretical procedure, utilizing calculations of atmospheric effects with a radiative transfer model, were used to adjust Day 1 signatures before they were applied to Day 2 data, and both procedures improved classification accuracy.

FORMERLY WILLOW RUN LABORATORIES, THE UNIVERSITY OF MICHIGAN

PROGRESS AND PLANS

Successful completion of the final aircraft MSS underflight of ERTS-1 was accomplished on September 6, 1973. The ERIM M-7 scanner was flown at several different altitudes over a 4-mile flight line that includes the Willow Run airport. Standard reflectance panels were deployed just off the airport ramp and a field crew made measurements of direct and diffuse irradiance (both spectral and broadband), sky radiance, and meteorological parameters.

One instrument deployed was the Bendix RPMI (Radiation Power Measuring Instrument) which was provided by Dr. Robert Rogers of the Bendix Aerospace Division who also cooperated on its use for measurements. Earlier in the year, we had used the instrument for other measurements and made a rather extensive set of calibration measurements on it. This calibration information has been reduced and tabulated. Both the procedures in the cali- bration and results obtained are presented in Appendix VII-1.

To date, we have been unsuccessful in ordering ERTS imagery and digital tapes for the Sept. 6, 1973, pass. Our standing order has elapsed and, due to a flaw in the first processed images, the job has been resub- mitted for image processing, according to GSFC personnel. Until it is processed and frame numbers identified, we cannot place our request.

The paper, described in earlier reports and entitled "Correlation of ERTS MSS Data and Earth Coordinate Systems," by W. Malila, R. Hieber, and A. McCleer, was presented at the Purdue Conference on Machine Processing of Remotely Sensed Data, Oct. 16-18, 1973. A copy is being forwarded separately to NTIS, and one was forwarded earlier to the Scientific Monitor of this task, Dr. Gerald Grebowsky.

A presentation of the progress, status, and significant results of the investigations being carried out under this task was made to the Interpre- tation Techniques Review Panel on October 24, 1973. We subsequently have been invited to present a paper at the December ERTS-1 Symposium and will do so.

We have carried out an initial exercise of our signature extension techniques on ERTS-1 data. Only recently did we obtain access to data sets suited for evaluation of the procedures. We need data on two different days over the same well ground-truthed site, with different amounts of haze present on the two days. A data set, being used in a study in which we are participating under the NASA SR&T program of the Johnson Space Center, met these criteria.

Classifier signatures were obtained for trees and crops on one day and applied directly in processing data from the preceding day. Classification performance was degraded because the different amount of haze present changed the magnitude and spectrum of the signals received by ERTS-1. By applying certain preprocessing procedures, we were able to adjust the signatures used, improve the classification performance, and, thereby, extend the original signature to the second day, hence the name, "signature extension". Two signature extension procedures were applied, one of an empirical nature and one of a theoretical nature.

To help describe the technique, the following example of tree recognition is given. First, an area that was 100% classified as trees on the first day was found and outlined on a recognition map. When the Day 1 signatures were applied to the Day 2 data, only 67% of the picture elements (pixels) were correctly classified as trees (symbol θ on Fig. VII-1). Then the signatures were adjusted by an amount determined by subtracting the mean level of signals over a larger nearby area on Day 1 from the mean levels computed for the same area on Day 2. A different adjustment was made for each channel. The adjusted signatures were used in the classifier and the classification percentage increased to 77% (Fig. 1(b)).

Photometer readings had been made on the two days at the time of the ERTS passes. These readings were used to calculate an optical depth at each wavelength for each day. Dr. Robert Turner of ERIM used his radiative transfer model to compute total radiance and path radiance quantities for those optical depths. We then computed signature adjustments based on the model calculations and applied them to the Day 2 data. The result, shown in Fig. 2(b), is that 85% of the pixels in the area were classified as trees. We plan to explore this data set in more detail to obtain a better understanding of the nature of atmospheric effects on classification accuracies and methods for alleviating these effects.
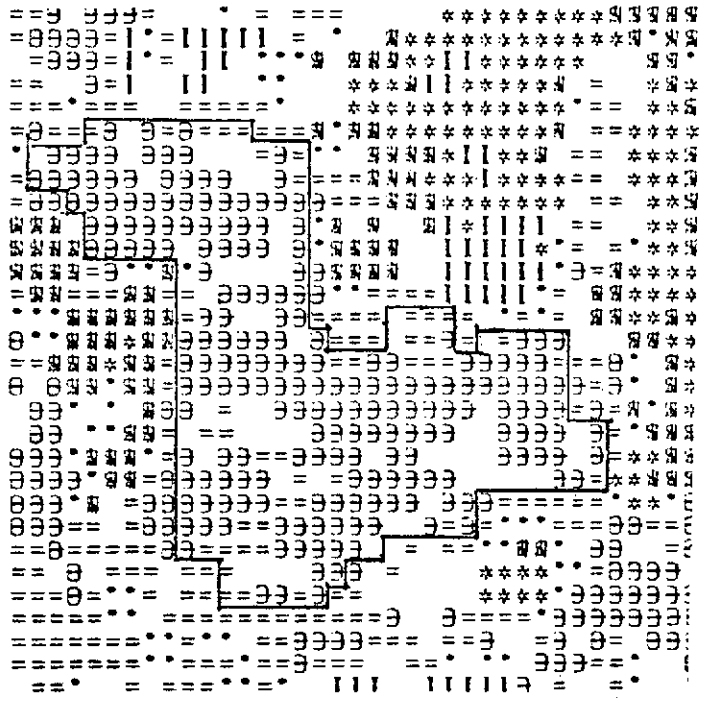
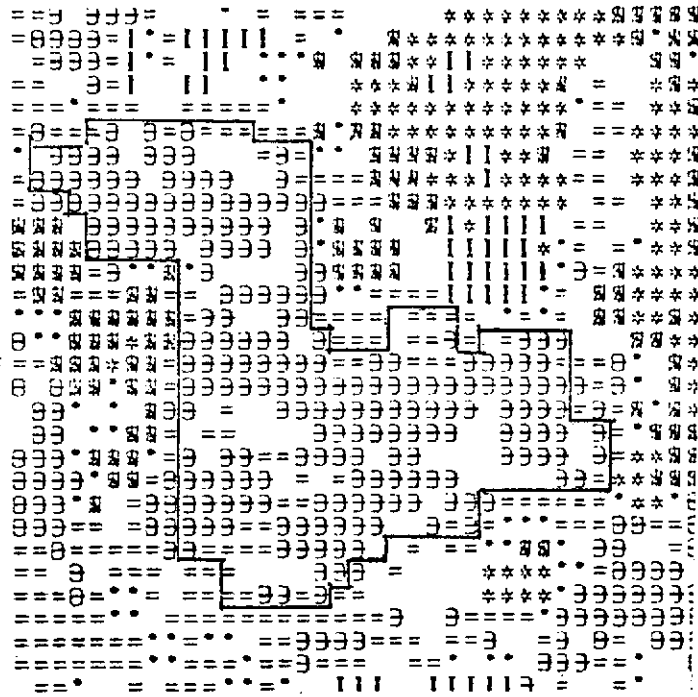(a) NO ADJUSTMENT OF SIGNATURES
(67% Called Trees)
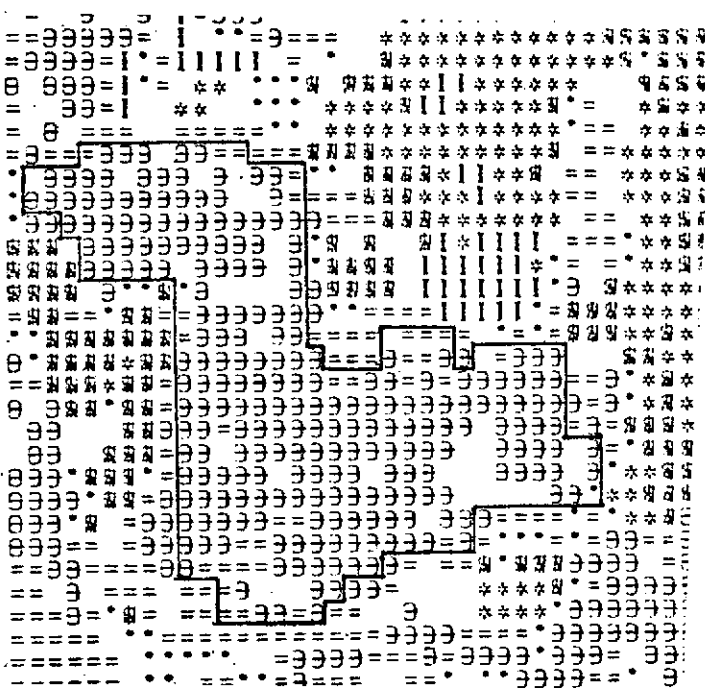
(b) AFTER EMPIRICAL MEAN LEVEL ADJUSTMENT OF SIGNATURES
(77% Called Trees)

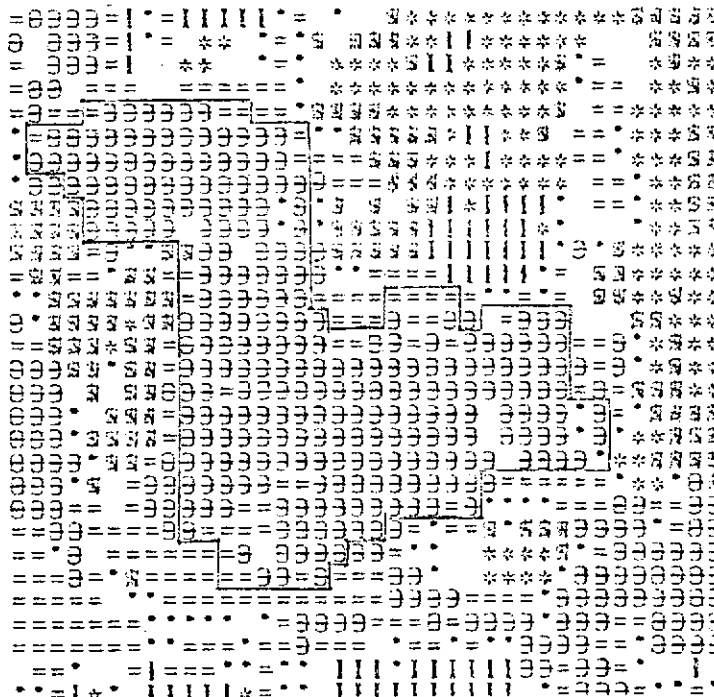EXAMPLE OF APPLYING SIGNATURES FROM ONE DAY TO DATA FROM PRECEDING DAY

EFFECT ON RECOGNITION OF TREES
(Outlined Area Completely Recognized
as Trees on Same Day as Signatures.)

FIGURE VII-1

ΣERIM

(a) NO ADJUSTMENT OF SIGNATURES
(67% Called Trees)

(b) AFTER THEORETICAL MEAN LEVEL ADJUSTMENT OF SIGNATURES
BASED ON PHOTOMETER READINGS AND MODEL
(85% Called Trees)

EXAMPLE OF APPLYING SIGNATURES FROM ONE DAY TO DATA FROM PRECEDING DAY

EFFECT ON RECOGNITION OF TREES
(Outlined Area Completely Recognized
as Trees on Same Day as Signatures.)

FIGURE VII-2

APPENDIX I

The Bendix RPMI (Radiant Power Measuring Instrument) is capable of making both radiance and irradiance measurements in four spectral regions in the visible and near infrared. The four spectral regions correspond to the ERTS MSS (Earth Resources Technology Satellite - MultiSpectral Scanner) bands 4, 5, 6, and 7. Figure 1 shows the relative spectral response of the RPMI for each of the four bands. (These data are from a Bendix bi-monthly progress report*.) Calibration measurements made at ERIM on one RPMI unit (S/N 100) are reported in this Appendix.**

The Bendix RPMI uses a transmissive diffuser to obtain a Lambertian, hemispherical, field of view. Since information was lacking on the angular response characteristics of the diffuser on the RPMI, measurements were made at ERIM to determine those characteristics. The data presented are normalized to the signal level at a zenith angle of 0° and also were corrected for the expected cosine response so that an ideal cosine receiver response would appear as a straight line with a magnitude of 1.0. The information is presented in a manner that indicates directly the difference between the ideal and real cosine receiver. The diffusivity measurements were made with the spectral band as a parameter. The data obtained are presented in Figures 2 through 5.

To make radiance measurements with the RPMI, a tube is installed over the cosine receiver, thus, restricting its field of view. While data were available giving the effective solid angle of the instrument in this configuration, there were no data on the angular response. Therefore, measurements were made at ERIM to determine the angular response using the four wavelength bands as parameters. These measurements were made using a source which has an extent of 1/2° (Note: the extent of the sun also is 1/2°). The data are presented in Figures 6 through 9. The angular responses presented are absolutely correct only when a source has an extent of 1/2° because of the source used. The measurements are the result of the convolution of the

*Report Period 1 April to 1 June 1973, Contract NAS5-21863, Experiment PR303.

**The work described in this Appendix was performed under Contract Number NAS5-21783, Task VII (MMC 136) for NASA's Goddard Space Flight Center, Greenbelt, Maryland.

BENDIX RPMI FILTERS

Figure 1

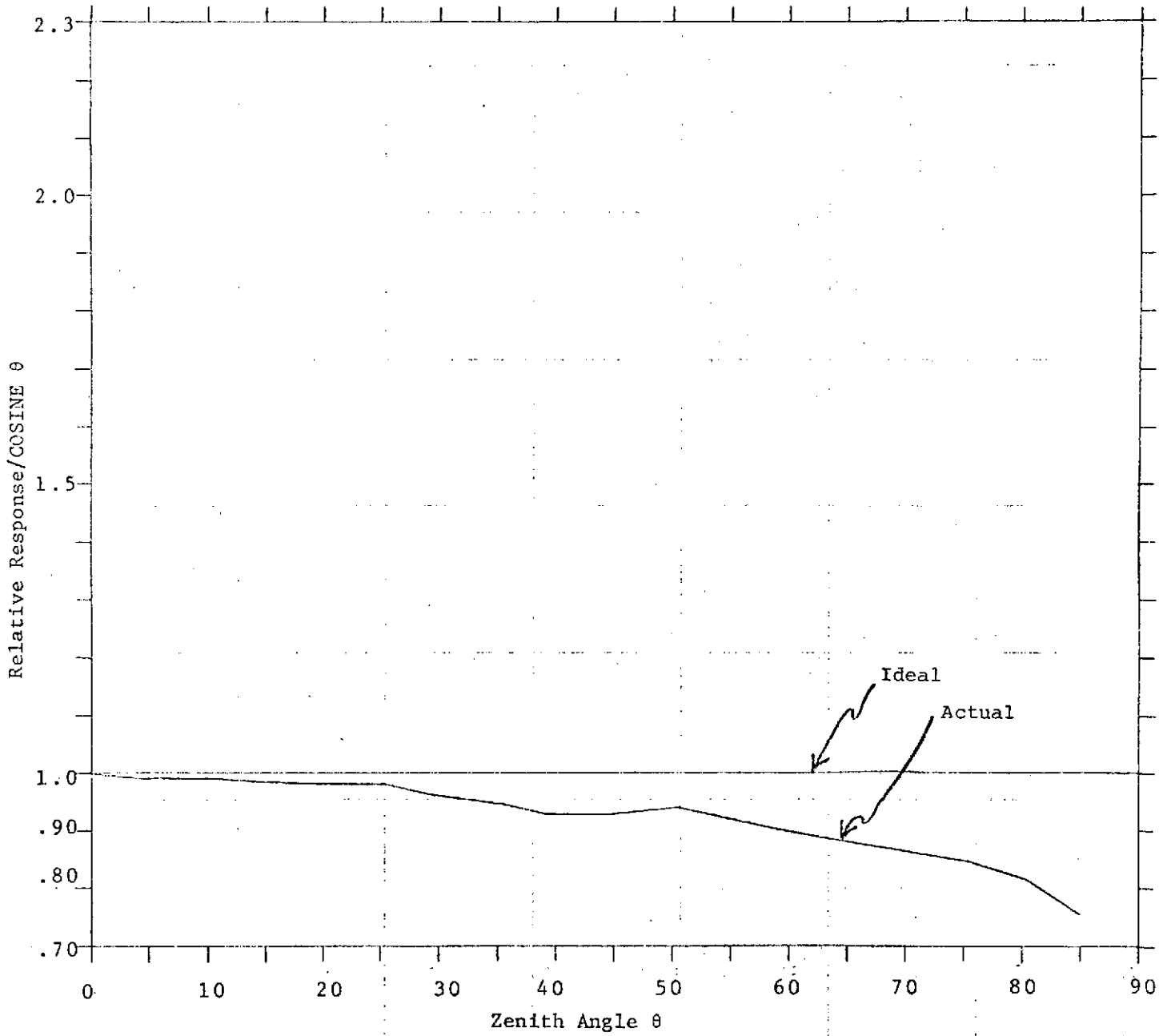|	ERTS	RPMI (and MMS)
	Band 4	Band 1
*	Band 5	Band 2
✱	Band 6	Band 3
✕	Band 7	Band 4

RELATIVE RESPONSE

WAVELENGTH

VII-7

34<
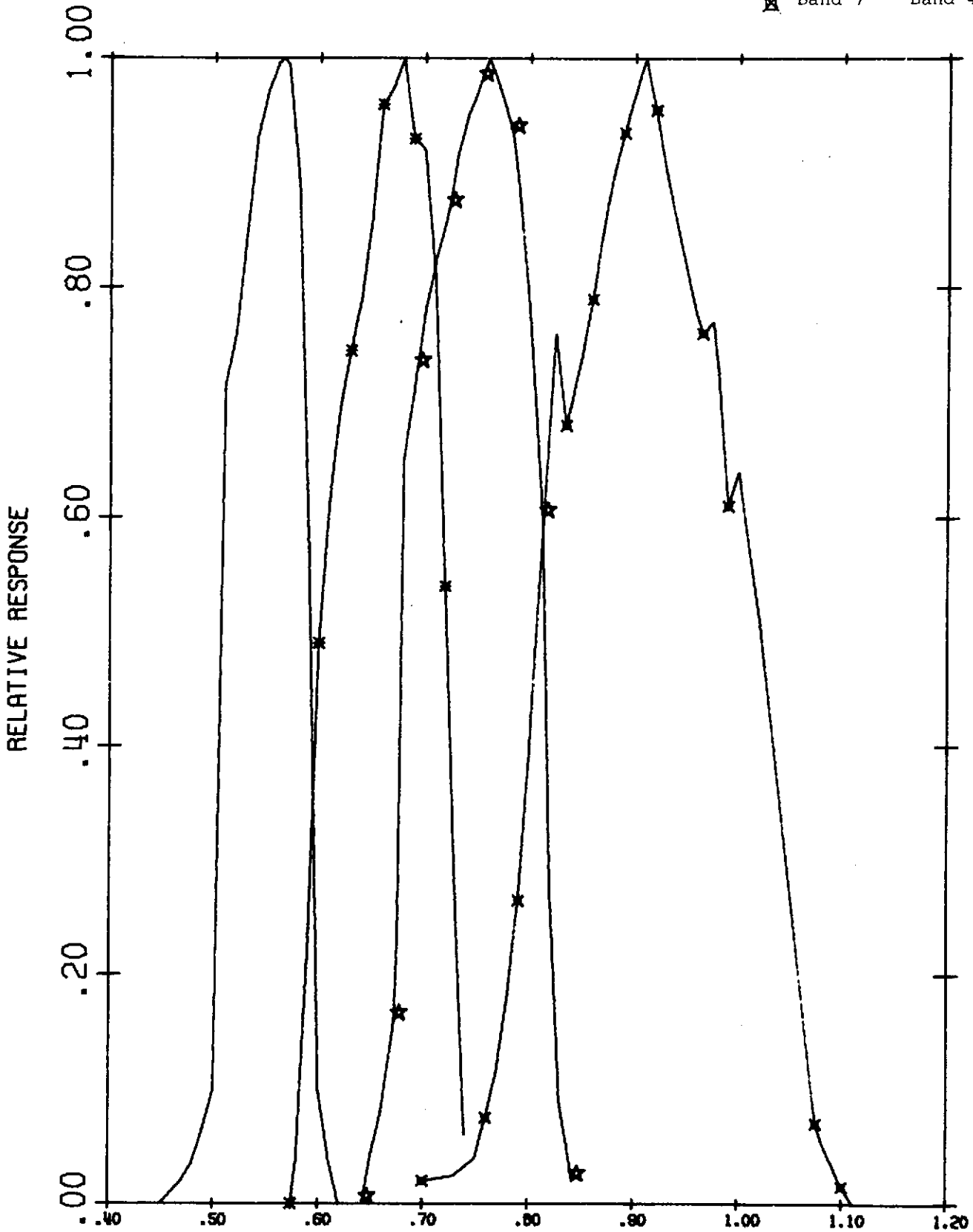
RELATIVE RESPONSE OF THE BENDIX RPMI's COSINE RECEIVER
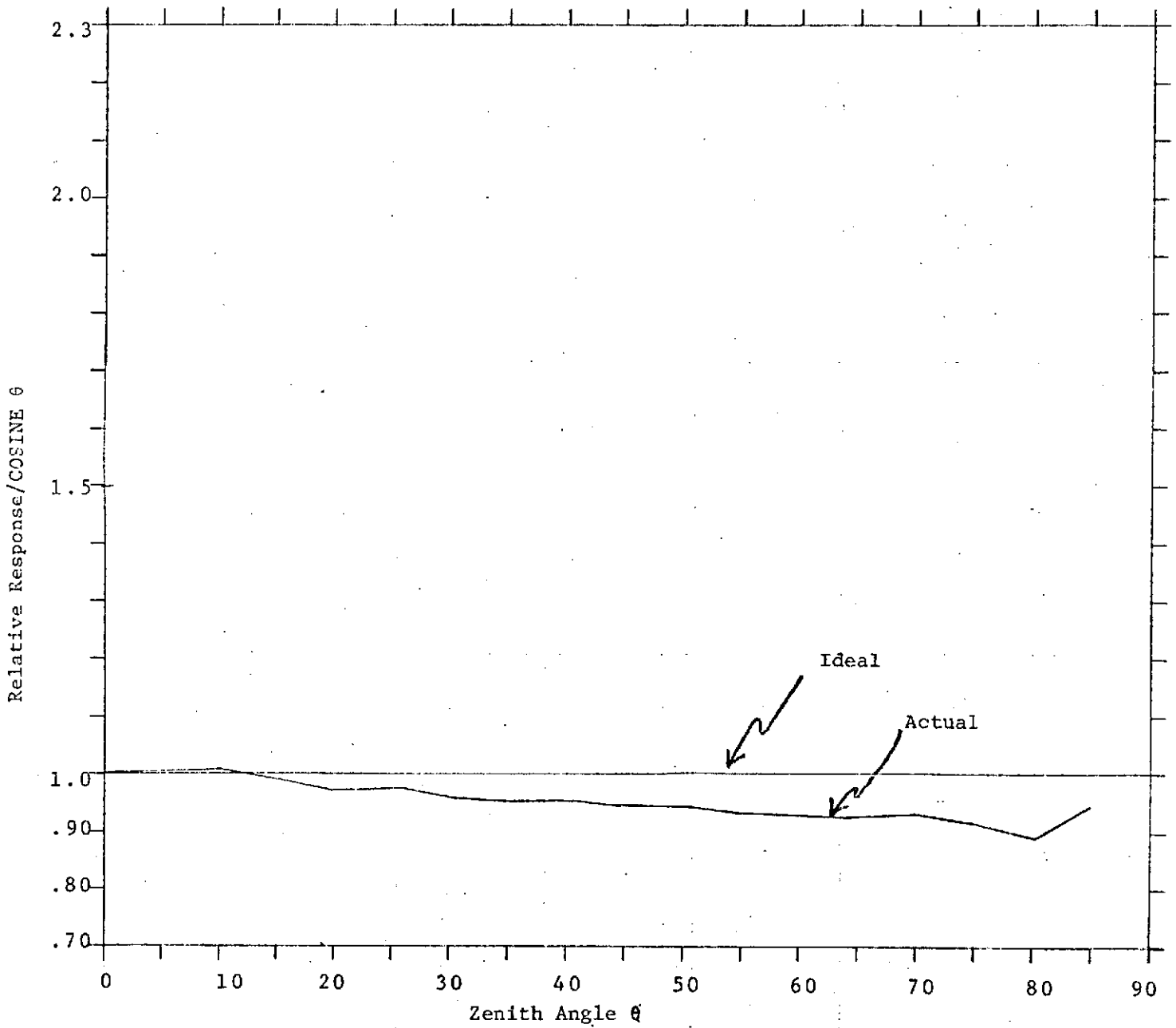
ERTS Band 4, or RPMI Band 1

Figure 2

35<

RELATIVE RESPONSE OF THE BENDIX RPMI's COSINE RECEIVER
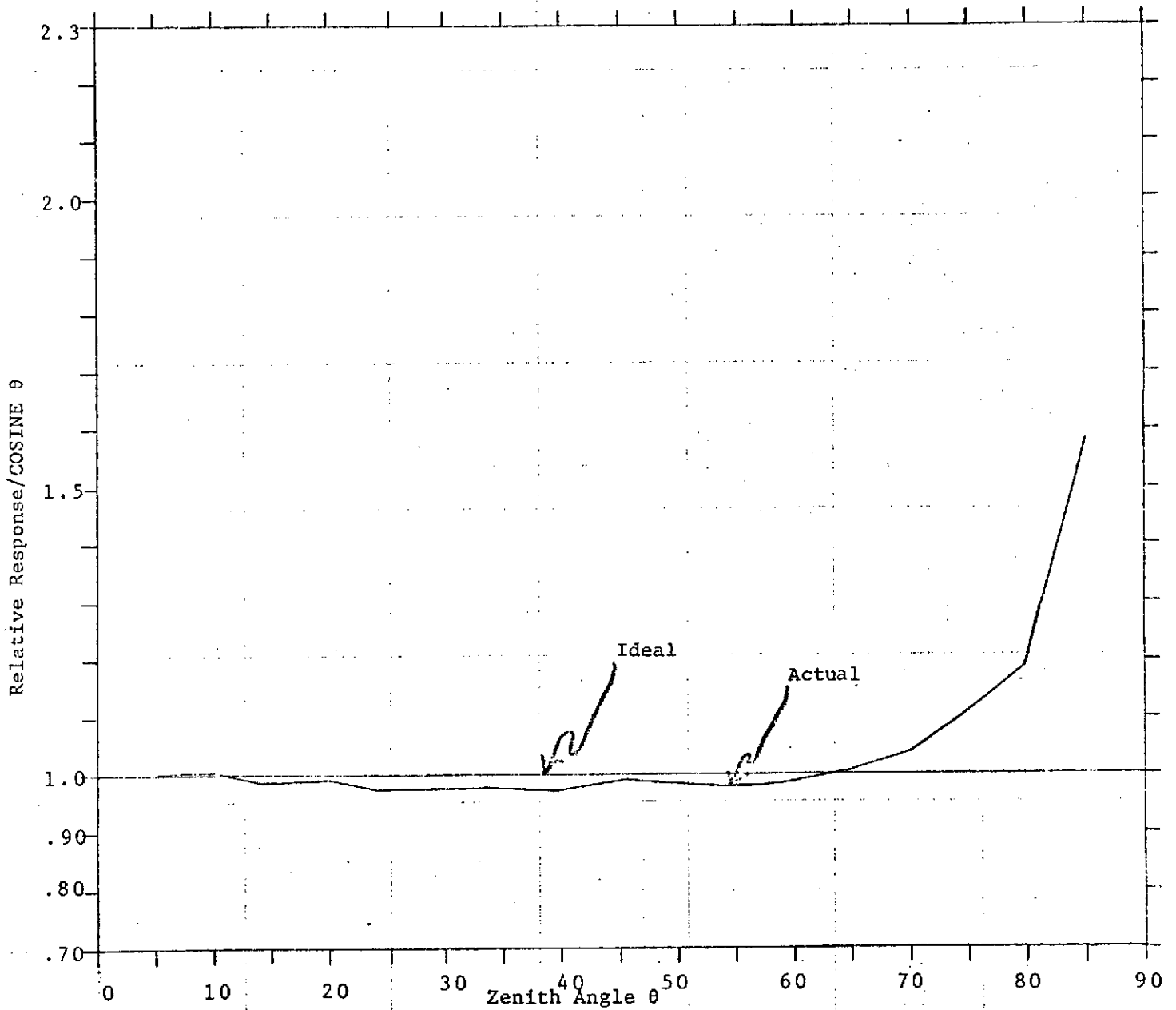
ERTS Band 5, or RPMI Band 2

Figure 3

RELATIVE RESPONSE OF THE BENDIX RPMI's COSINE RECEIVER
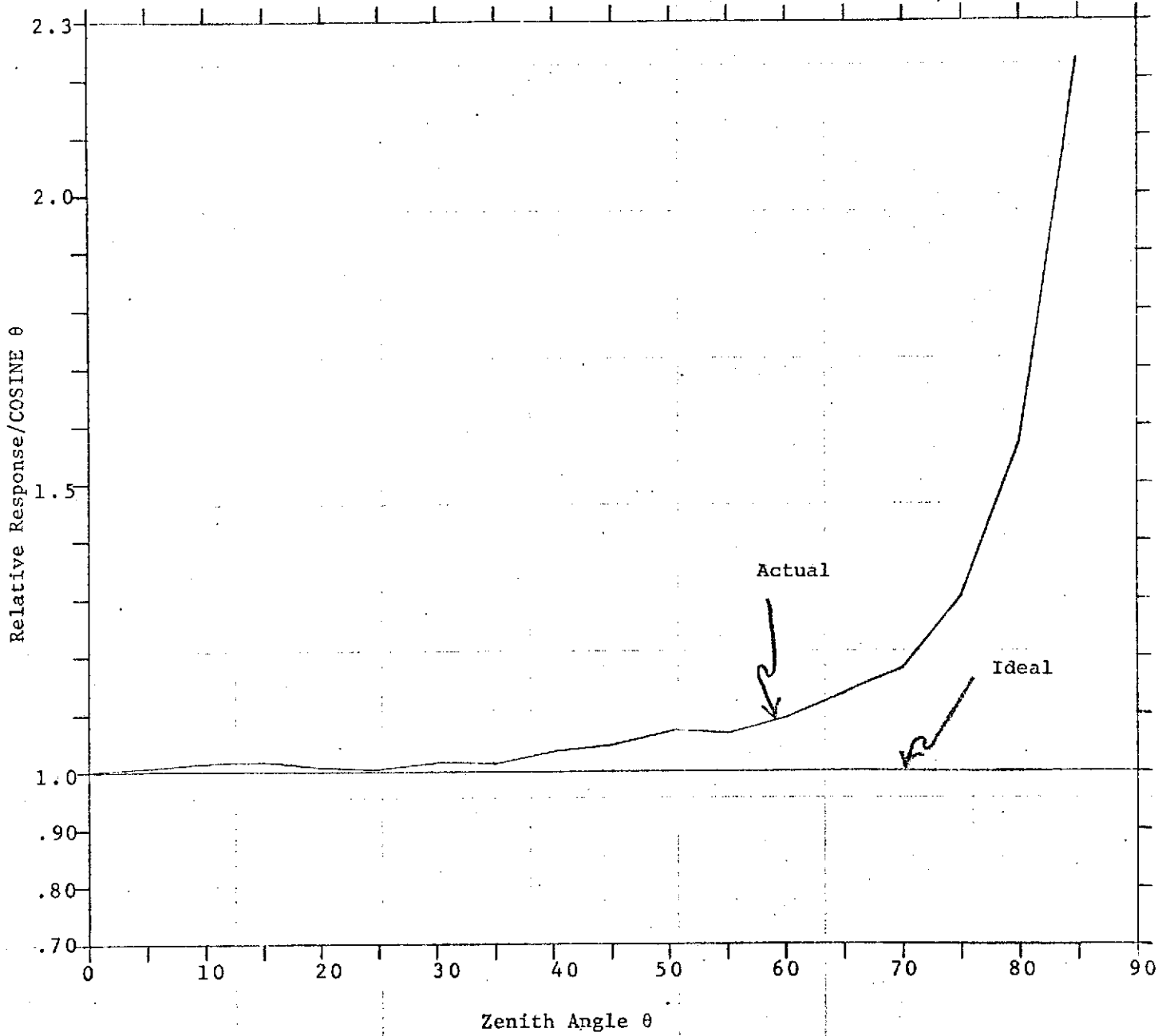
ERTS Band 6, or RPMI Band 3

Figure 4

RELATIVE RESPONSE OF THE BENDIX RPMI's COSINE RECEIVER

ERTS Band 7, or RPMI Band 4

Figure 5

Zenith Angle θ

VII-11

∑ERIM

1/2° source with the actual angular response of the instrument. An example of the smoothing produced by an extended source is illustrated in Figure 10. The example shows how a particular angular response is affected by being smoothed with a source having an extent of 1°.

Independent radiance and irradiance calibrations were also made by ERIM personnel. The objective of radiometer calibration is to establish an accurate relationship between the output signal, S, and the irradiance or radiance within the spectral band of operation of the radiometer. That is,

$$S = R_E E(\lambda_1 \text{ to } \lambda_2)$$

for irradiance (E) and

$$S = R_L L(\lambda_1 \text{ to } \lambda_2)$$

for radiance (L) where the proportionality constants R_E and R_L are to be determined and λ_1 and λ_2 are the band limits.

The band of operation is found for each radiometer channel by normalizing the respective relative spectral responsivities $r(\lambda)$ to the peak. Thus,

$$\Delta\lambda = \int_0^\infty r(\lambda)d\lambda$$

determines the bandwidth, $\Delta\lambda$, and

$$\overline{\lambda}\Delta\lambda = \int_0^\infty \lambda r(\lambda)d\lambda$$

determines the band center, $\overline{\lambda}$. Therefore, the band limits, λ_1 and λ_2, are

$$\lambda_1 = \overline{\lambda} - \Delta\lambda/2$$

$$\lambda_2 = \overline{\lambda} + \Delta\lambda/2$$

The values of R_E and R_L can be determined by exposing the radiometer to a source providing a known spectral irradiance or radiance and observing the resulting signal.
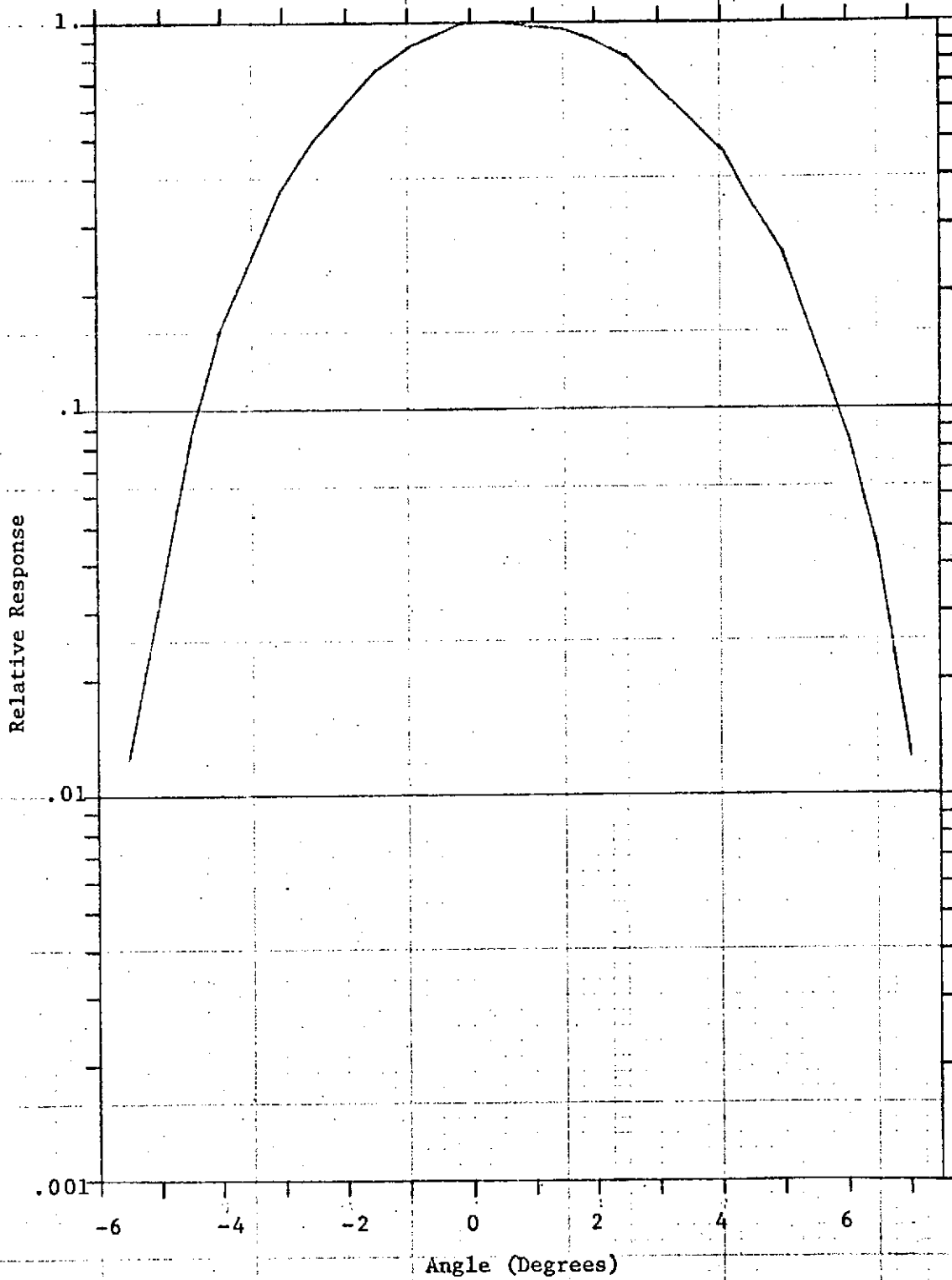
Thus,

(1) $R_E = S(\text{observed})/E(\lambda_1 \text{ to } \lambda_2)$

(2) $R_L = S(\text{observed})/L(\lambda_1 \text{ to } \lambda_2)$

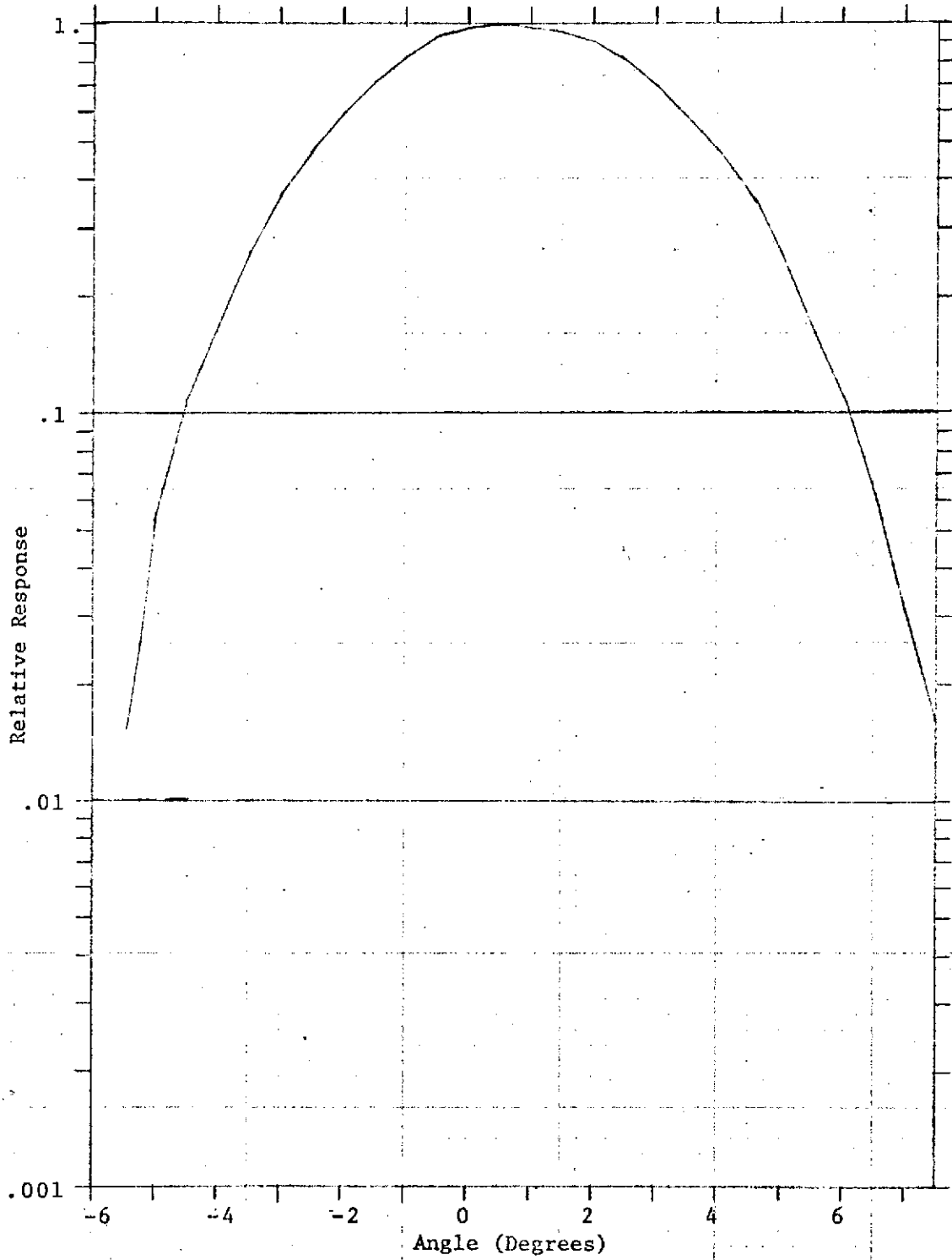RELATIVE RESPONSE OF BENDIX RPMI
ERTS Band 4, RPMI Band 1

Figure 6

VII-13

40<

RELATIVE RESPONSE OF BENDIX RPMI
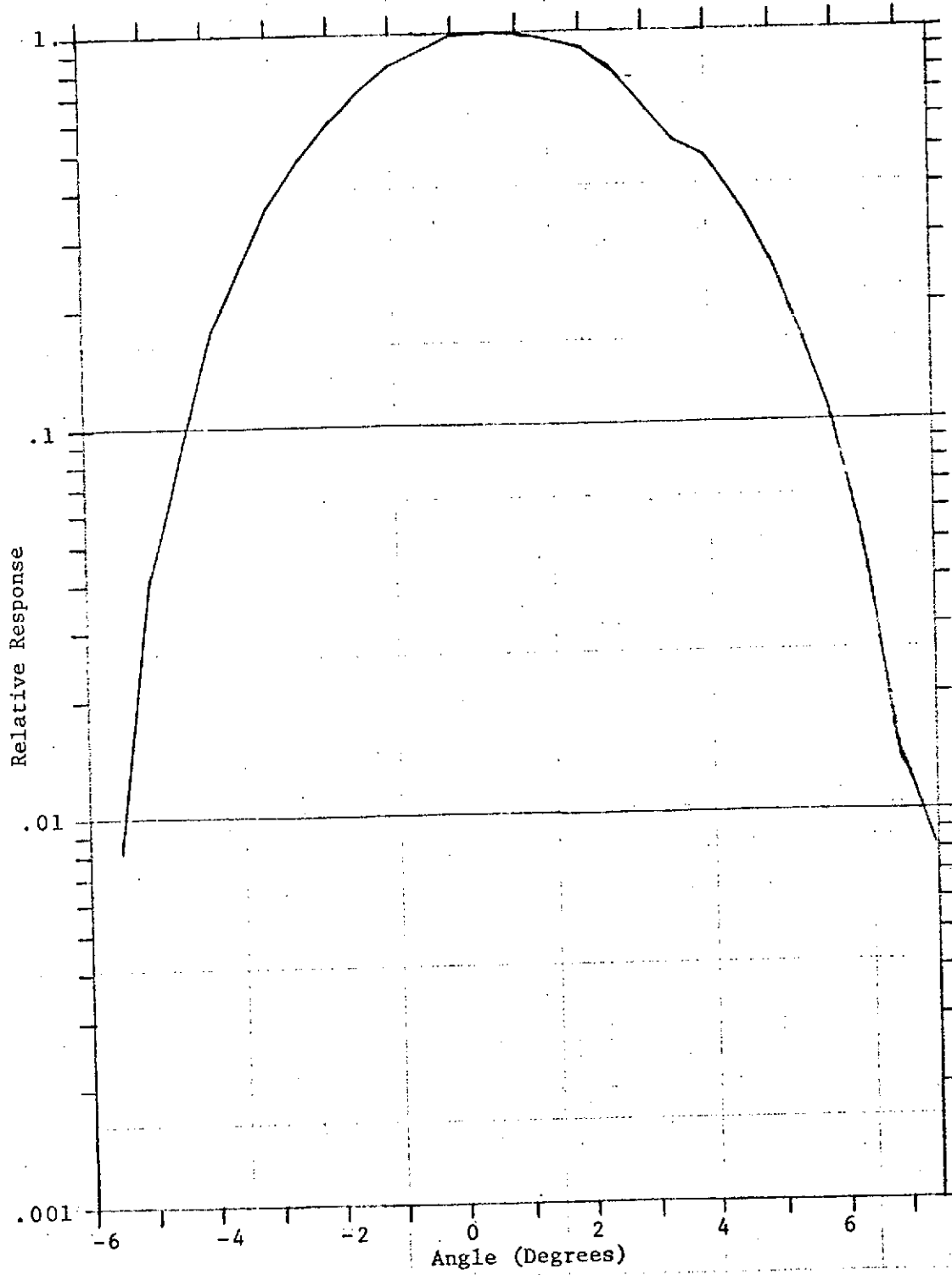
ERTS Band 5, RPMI Band 2

Figure 7

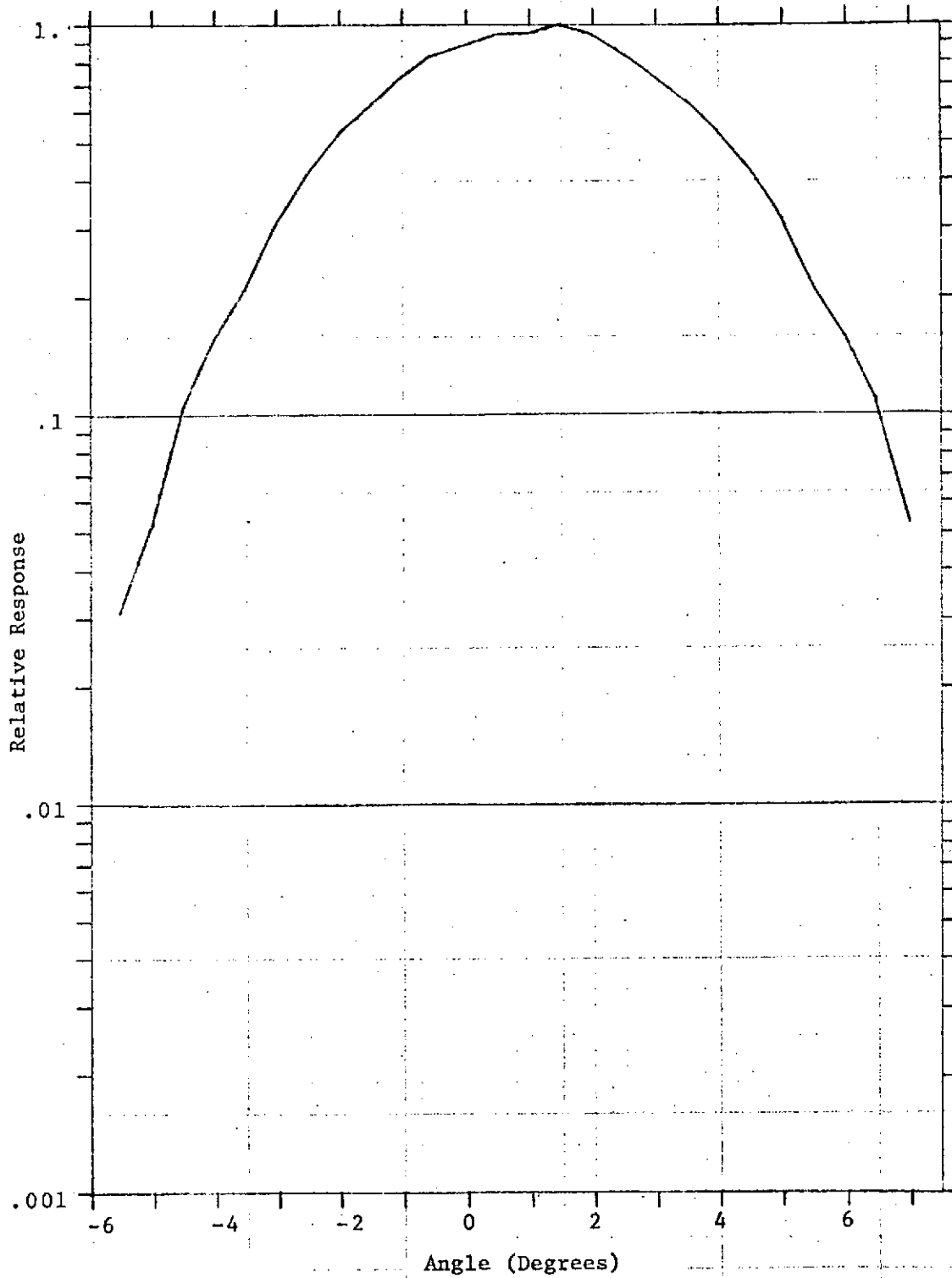RELATIVE RESPONSE OF BENDIX RPMI

ERTS Band 6, RPMI band 3

Figure 8

RELATIVE RESPONSE OF BENDIX RPMI
ERTS Band 7, RPMI Band 4

Figure 9

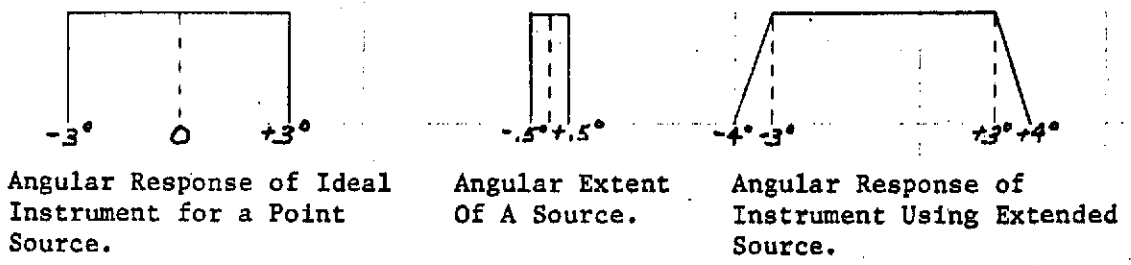Angular Response of Ideal   Angular Extent   Angular Response of
Instrument for a Point   Of A Source.   Instrument Using Extended
Source.   Source.

Figure 10

⟩ERIM
_____

where $E(\lambda_1$ to $\lambda_2)$ and $L(\lambda_1$ to $\lambda_2)$ are found by numerical integration of the known spectral irradiance or radiance between the band limits λ_1 and λ_2.

If one assumes that the radiometer responds linearly with incident flux, then the exact relationship between output signal and the irradiance or radiance in the band of operation has been found for all sources which have the same spectral distribution as the calibration source.

The proportionality constants in Equations 1 and 2 are correct only for a target that has the same relative spectral irradiance or radiance as the calibration source. The source used for the calibration was a tungsten lamp, and since the instrument is used outdoors, it is desired to find the relationship for sunlight, the spectral distribution of which is markedly different from that of a tungsten source. Also, the spectrum of sunlight at ground level is different from that outside the atmosphere, and can vary throughout a day and from day to day.

The signal, $S(sun)$, could be calculated (instead of observed) by the relation

$$S(sun) = R_E(peak) \int_O^\infty r(\lambda) E_\lambda(sun) d\lambda$$

and, hence, the required constant, $R_E(sun)$ could be determined by

$$R_E(sun) = R_E(peak) \int_O^\infty r(\lambda) E_\lambda(sun) d\lambda / E(\lambda_1 \text{ to } \lambda_2, sun)$$

if the value of $R_E(peak)$ were known. Values for $E_\lambda(sun)$ are tabulated in references or can be calculated. (Note: The relative spectral irradiance of the source may be used because the ratio

$$\int_O^\infty r(\lambda) E_\lambda(\lambda) d\lambda / E(\lambda_1 \text{ to } \lambda_2)$$

is independent of the absolute magnitude of $E_\lambda(\lambda)$.) The results of a calibration experiment with a tungsten standard lamp allow the value of $R_E(peak)$ to be computed since

$$S = R_E(tung) E(\lambda_1 \text{ to } \lambda_2, tung) = R(peak) \int_O^\infty r(\lambda) E_\lambda(tung) d\lambda.$$

Consequently,

$$R(\text{peak}) = \frac{R_E(\text{tung})E(\lambda_1 \text{ to } \lambda_2, \text{tung})}{\int_0^\infty r(\lambda) \, E_\lambda(\text{tung}) d\lambda}$$

Therefore, by substitution

$$R_E(\text{sun}) = \frac{\int_0^\infty r(\lambda)E_\lambda(\text{sun})d\lambda / E(\lambda_1 \text{ to } \lambda_2, \text{ sun})}{\int_0^\infty r(\lambda)E_\lambda(\text{tung})d\lambda / E(\lambda_1 \text{ to } \lambda_2, \text{ tung})} R_E(\text{tung})$$

The relation

$$S = R_E(\text{sun})E(\lambda_1 \text{ to } \lambda_2, \text{ sun}),$$

is the desired exact relationship between output signal and irradiance in the band of operation for all sources which have the same spectral distribution as sunlight.

A suitable constant of proportionality may be derived for any other kind of spectral distribution in the same way as for sunlight.

In general, if one defines a source constant, $K_E(i)$, for the ith source as

$$K_E(i) = \int_0^\infty r(\lambda)E_\lambda(i,\lambda)d\lambda / E(\lambda_1 \text{ to } \lambda_2, i).$$

then the relation between the values $R_E(i)$ and the $R_E(\text{calibration})$ is

$$R_E(i) = \frac{K_E(i)}{K_E(\text{calibration})} R_E(\text{calibration})$$

and the exact relationship between output signal and irradiance in the band of operation is

$$S = R_E(i)E(\lambda_1 \text{ to } \lambda_2, i).$$

When the spectral distribution is not known, the best overall compromise value for R_E is $R_E(\text{peak})$, to yield the best overall accuracy.

The irradiance calibration was performed using a standard of spectral irradiance. The radiance calibration was accomplished using a reflecting panel of 3M White Paint illuminated by a standard of spectral irradiance which is traceable to NBS. The calibration constants were evaluated using Equation

ΣERIM

1, for the irradiance constants, and Equation 2, for the radiance constants. Table I contains the calculated values of the reciprocals of the proportionality constants R_E(peak), R_L(peak), R_E, and R_L for each of the RPMI bands. The reciprocals are given because calibration constants are conventionally given as multiplicative constants (i.e. in data reduction the expression to be evaluated is $E(\lambda_1 \text{ to } \lambda_2) = S\ R_E^{-1}$ where S is the meter reading, and R_E is the calibration constant).

The calibration constants presented in Table I cannot be compared directly with the calibration constants reported by Bendix because Bendix used a different calibration procedure and reported the reduced data in a different set of units. The differences between the calibration procedures and units have not yet been reconciled.

Table II gives the values of $\Delta\lambda$ and $\overline{\lambda}$ as well as the constant K(calibration) for the calibration sources.

TABLE I

RPMI Band / ERTS Band	$(R_E\text{peak})^{-1}$ $\left(\dfrac{MW\text{-}cm^{-2}}{unit}\right)$	$(R_L\text{peak})^{-1}$ $\left(\dfrac{MW\text{-}cm^{-2}\text{-}ster^{-1}}{unit}\right)$	$(R_E)^{-1}$ $\left(\dfrac{MW\text{-}cm^{-2}}{unit}\right)$	$(R_L)^{-1}$ $\left(\dfrac{MW\text{-}cm^{-2}\text{-}ster^{-1}}{unit}\right)$
1 4	.894	64.1	.847	60.7
2 5	1.130	80.1	1.198	84.9
3 6	1.35	93.4	1.471	101.8
4 7	1.928	133.5	1.799	124.6

$$E_i = S_i R_{E_i}^{-1} \quad \text{and} \quad L_i = S_i R_{L_i}^{-1}$$

E_i = Irradiance in Band i

L_i = Radiance in Band i

S_i = Meter reading for Band i

$R_{E_i}^{-1}$ and $R_{L_i}^{-1}$ = Irradiance and radiance calibration constants for Band i.

TABLE II

RPMI Band	$\Delta\lambda$ [μm]	$\overline{\lambda}$ [μm]	Irradiance Standard		Radiance Standard		$K_E = \dfrac{\int_o^\infty r(\lambda)E(\lambda)d\lambda}{E(\lambda_1 \text{ to } \lambda_2)}$	$K_L = \dfrac{\int_o^\infty r(\lambda)L(\lambda)d\lambda}{L(\lambda_1 \text{ to } \lambda_2)}$
			$E(\lambda_1 \text{ to } \lambda_2)$ mw-cm^{-2}	$\int_o^\infty r(\lambda)E(\lambda)d\lambda$ mw-cm^{-2}	$L(\lambda_1 \text{ to } \lambda_2)$ mw-cm^{-2}-ster^{-1}	$\int_o^\infty r(\lambda)L(\lambda)d\lambda$ mw-cm^{-2}-ster^{-1}		
1	.080	.550	.206	.195	.0566	.0536	.947	.947
2	.109	.664	.426	.452	.117	.124	1.06	1.06
3	.124	.748	.612	.668	.168	.184	1.09	1.09
4	.196	.925	1.20	1.12	.329	.307	.933	.933

ΣERIM

Seventh Type I Progress Report – 1 September 1973 – 31 October 1973
Task VIII – Water Quality Monitoring – 1400
C.T. Wezernak, UN 625, MMC 081

Work during the reporting period has been initiated towards defining the quantitative relationship observed between suspended solids (Total Non-filtrable Residue) and digital integer level in MSS 5.

A statistical analysis of all four bands has been carried out for the New York Bight data, 1258-15082 (7 April 1973) and 1024-15071 (16 August 1972). These data are being used to determine minimum detectable concentrations of materials, expressed as suspended solids.

Digital processing of Lake Erie frames 1247-15481 (27 March 1973) and 1319-15474 (7 June 1973) has been performed. Analysis of individual lines at two selected transects has also been performed to determine correlation between digital integer level in MSS 5 and relative concentration of suspended solids. Work is in progress to normalize results obtained on the above two dates. A similar analysis of Lake Erie data is planned for frames 1265-15480 (14 April 1973), 1337-15472 (25 June 1973), and 1355 (13 July 1973). Digital tapes for the above dates have been ordered.

Digital processing has been initiated on portions of frames 1321-15590 and 1321-15584 (9 June 1973) Lake Michigan. These last two show the spread of water masses from the highly industrial Burns Ditch area of Indiana and "thermal bar" (color anomaly) formation in the Muskegon area.

Plans for the next bi-monthly period include completion of processing of Lake Erie data and Lake Michigan data.

ΣERIM

Seventh Type I Progress Report - 1 September 1973 - 31 October 1973
Task IX - Oil Pollution Detection - 1389
R. Horvath - UN 606, MMC 079

Digital data processing of MSS frames 1183-18175 and 1184-18234 has
been completed. These frames imaged the 120,000 gal. waste oil spill
at Oakland, California in January 1973. Processing has shown that radiance
anomalies exist in bands 4, 5, and 6 at the approximate spatial locations
of the slick as reported by the U.S. Coast Guard. However, these anomalies
are spectrally and quantitatively indistinguishable from natural suspended
solids anomalies occurring in the area due to tidal cycling. Thus, while
we may have detected the oil slick, we certainly cannot state that we
have recognized it as such.

MSS imagery of the Monongahela River oil spill of June 1973 (frame
1317-15363) and of natural oil seepage in the Santa Barbara Channel
(frame 1325-18072) have been received. Interpretation of the Monongahela
River images shows no detectable sign of any oil slick. In fact, the
river is so narrow (in comparison to ERTS spatial resolution) that even
a very intense slick would probably be undetectable due to the relatively
low contrast of oil on water. The Santa Barbara frame is uninterpretable
due to the presence of heavy fog in the affected area.

We are continuing to keep abreast of plans for a major (500,000 gal.)
intentional oil spill to be created in the Atlantic Ocean in March 1974.
This is a research oriented project being conducted by the U.S. Coast
Guard and American University with support from other organizations.
Assuming continued operational status for the ERTS-1 MSS, coverage of this
slick would provide the necessary data to meet the major objectives of
this task.

ᗡERIM

Seventh Type I Progress Report - 1 September 1973 - 31 October 1973
Task X - An ERTS Experiment for Mapping Iron Compounds - 1383
R.K. Vincent, UN 422, MMC 075

The general objectives of this investigation are to develop
quantitative methods for mapping lithologic units strongly
associated with iron oxides, and to use this method to map iron
oxides in the vicinity of the Wind River Range, Wyoming.

Careful analysis of the automatic recognition map of ERTS frame
E-1013-17294 is in progress, uniting information from ground truth,
literature, the geologic map, and communications with geologists who
have worked in the area. The five target classes included in the
recognition map (shown in different colors on figure 1) result from
training on 5 known areas on the southeastern edge of the Wind River
Range. These targets were all within the groundtruth area, a region
approximately 100 sq. mile, or 1% of the total area of the area
mapped. The targets were:

1) Triassic redbeds
2) Phosphoria formation
3) Granite of the Luis Lake Batholith
4) Limestone
5) Iron ore in Atlantic City Iron Mine,
   U.S. Steel Corporation

In order to determine exactly what compositional differences are
being detected by the recognition process, the first step was to test
to what degree recognition is controlled by geology. In other words,
how well does recognition match the geologic map. Using the USGS
Geologic Map of Wyoming, 1952, for a base map, we first noted the color
that specific formations in the ground truth area were recognized as and
then noted how well the automatic recognition matched the outlines of the
formations as they appear on the map. The formations were then followed
throughout the scene to test the consistency of recognition. Some
formations were well recognized as one target throughout; others were
recognized only locally. However, a formation recognized as two different
targets in two different areas of the scene does not necessarily constitute
an inaccuracy. Actual compositional differences in formations mapped as
a single unit can be the cause of recognition differences. Only after
complete evaluation of the stratigraphy through a literature search and
careful examination of consistencies and inconsistencies will we be
able to evaluate the success of this procedure.

Two formations of particular interest are the Chugwater formation
(the name used as a general term for Triassic redbeds) and the Tertiary
Wind River formation. The two formations show the extremes of consistent
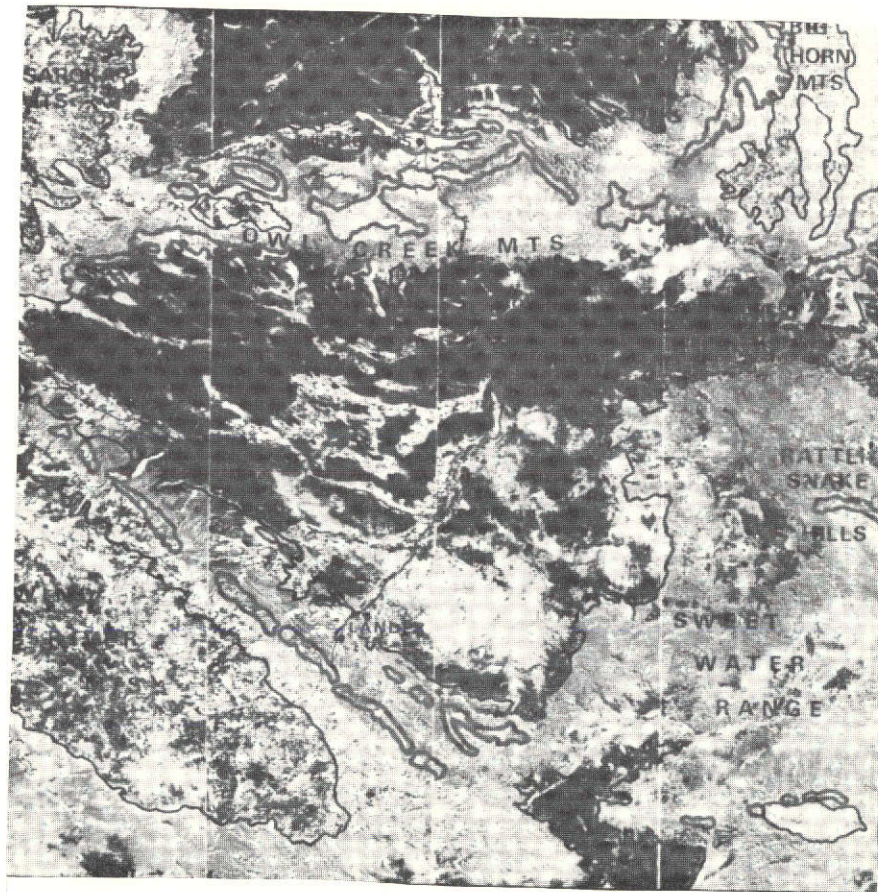and inconsistent recognition. As illustrated in Figure 1 in which red

ΣERIM

FIGURE 1. "Five Class lithologic map produced using 6 ratios of ERTS MSS data"

ΣERIM

recognition closely conforms to the superimposed outline of formation boundaries (USGS geologic map, 1952), redbeds can be easily separated from other lithologic types throughout the scene. However, within the formation boundaries of the Wind River formation, local recognition of blue, orange, or purple is evidenced. We are presently investigating the possibilities for these differences. The Wind River formation is the well known host rock of uranium deposits often accompanied by colorful alteration products. Differences could possibly be correlated with such alteration, or perhaps with lithologic differences of member units.

A preliminary look at rock types recognized in different target classes has resulted in the following summary keyed to figure 1:

Red	Hematitic sediments and red pyroclastics
Violet	Variegated shales, claystones, and dolomitic silt
blue	Gray shales, gray sandstones, relatively fresh granite
orange	Buff-colored limestones, sandstones, and weathered granite
black	Magnetite and amphibole-rich rocks
green	Dense vegetation

After completion of our literature search and study of stratigraphic and recognition correlation, it will be possible to say more about the potential techniques for reconnaisance mapping and mineral exploration.

∑ERIM

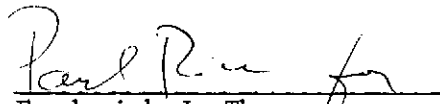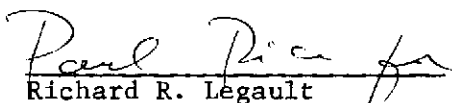FORMERLY WILLOW RUN LABORATORIES. THE UNIVERSITY OF MICHIGAN

TASK VIII - Work is being directed to the definition of the relationship between suspended solids as determined from water samples and the ERTS MSS Band 5 data. Analysis has been conducted for two frames covering the New York Bight area. Digital processing has been performed for two Lake Erie frames. Processing of two frames for Lake Michigan is underway (Indiana coast and the Muskegon, Michigan, areas).

TASK IX - Digital processing of two frames which imaged an oil spill area at Oakland, California,was completed. MSS imagery of an oil spill in the Monongahela River (Pennsylvania) did not show any sign of oil slick (river was narrow in relation to ERTS resolution). Fog covered a Santa Barbara frame so that oil seepage could not be observed. The task is keeping in touch with plans for an experimental oil spill in the Atlantic Ocean (March 1974).

TASK X - Detailed analysis of ERTS frame E-1013-17294 is continuing. Five target classes have been included in a recognition map, which includes formations related to iron oxides. This map is presented as a figure in this report. In this map the Chugwater formation appears to be mapped consistently while the Tertiary Wind River formation exhibits inconsistencies in its mapping. These differences are being investigated. With literature search and further analysis it is expected that reconnaissance mapping and mineral exploration techniques can be discussed in terms of the ERTS data potential for such investigations.

Respectfully submitted,

Frederick J. Thomson
Research Engineer

Approved by:

Richard R. Legault
Director, Infrared and Optics
Division

FJT/RRL/dlc

Attachments:
      List of Tasks
      List of current papers from the Tasks
      Type I reports for each of the ten tasks